NSS
Neutrosophic Sets and Systems, Vol. 79, 2025
University of New Mexico

Numerical and Semi Analytical Scheme for developing a solution to Falkner Skan equation in Neutrosophic environments

B. Amudha[1], M. Shanmugapriya[2], R. Sundareswaran[3*], Said Broumi[4]

[1, 2,3]Department of Mathematics, Sri Sivasubramaniya Nadar College of Engineering, Chennai - 603 110, India

[1]Laboratory of Information Processing, Faculty of Science Ben M'Sik, University of Hassan II, Casablanca, Morocco

Email: shanmugapriyam@ssn.edu.in, sundareswaranr@ssn.edu.in, s.broumi@flbenmsik.ma,

**Corresponding author detail: sundareswaranr@ssn.edu.in*

Abstract: This study presents a detailed analysis of the Falkner-Skan equation under uncertainty by employing neutrosophic numbers to represent the uncertainty in no slip conditions and the parameter $\tilde{\lambda}$. By applying appropriate similarity transformation, partial differential equation (PDE) are converted into ordinary differential equation (ODE). Both the Shooting Method and the Homotopy Perturbation Method (HPM) are utilized to solve ODE's. These ODE's are then transmuted into neutrosophic differential equation (NDE) by employing $(\tilde{A}, \tilde{B}, \tilde{\Gamma})_{cut}$ approach. The parameter $\tilde{\lambda}$ and no slip conditions are taken as triangular and trapezoidal neutrosophic numbers. The results are presented graphically to illustrate the comparative effectiveness of these methods. The analysis reveals that use of trapezoidal neutrosophic numbers and triangular neutrosophic numbers in Falkner-Skan equation gives strong neutrosophic solution. A 3D error analysis is conducted to compare the performance of triangular and trapezoidal neutrosophic numbers, highlighting their relative accuracy in solving the Falkner-Skan equation under varying degrees of uncertainty.

Keywords: Falkner-Skan Equation; Neutrosophic set; Triangular Neutrosophic Number; Trapezoidal Neutrosophic Number; Homotopy Perturbation Method.

1. Introduction

Classical set theory is widely applied in various real-world contexts to organize, categorize, and analyze information. A classical set incorporates elements that satisfy factual membership properties. Fuzzy set theory is an extension of classical set theory popularized by Zadeh [1] in 1965 that deals with uncertainty and imprecision. It is highly effective in controlling ambiguities emerging from an element's vagueness in a set, although it is incapable to simulate all forms of uncertainty encountered in various real-world physical problems with incomplete information. The abstraction of fuzzy set is recognized as Intuitionistic fuzzy sets invented in 1986 by Atanassov [2–5]. Each element in Intuitionistic fuzzy set has membership and non-membership values where their sum is greater than or equal to one. Later, in 1998, Smarandache [6–8] introduced Neutrosophic set theory, further generalizing classical, fuzzy, and intuitionistic fuzzy set theories. It is designed to handle various types

of uncertainties, including incomplete, indeterminate, and inconsistent information in real world. They are characterized by three membership functions: truth, falsity, and indeterminacy, each of which can take values in the range $]0^-,1^+[$.

Differentiation is crucial in science and engineering for modeling and solving various problems involving rates of change. Many real-world problems come with uncertain or imprecise parameters, which traditional differential equations struggle to handle. Fuzzy differential equations (FDE) handle uncertainty by representing variables with fuzzy sets. Bede et al. [9] investigated first order linear FDE's under various interpretations and demonstrated that the behavior of the solutions varies depending on the interpretation used. Vasavi et al. [10] applied fuzzy logic to Newton's law of cooling using different interpretations of fuzzy differential equations. They utilize a specific mathematical method (variation of constants) to find solutions that can better reflect the actual behavior of systems under uncertainty. Further, to improve upon fuzzy differential equations, intuitionistic fuzzy differential equations were developed. Ettoussi et al. [11] explored how intuitionistic fuzzy differential equations can be solved uniquely and exist using method of successive approximation and discusses the continuity of these solutions in the context of fuzzy set theory. In engineering, science, economics, and other fields, many systems are influenced by factors that cannot be precisely measured or predicted. Neutrosophic differential equations allow for a more accurate and realistic modeling of these systems by capturing all facets of uncertainty. Moi et al. [12] has examined second order boundary value problem through neutrosophic differential equation. Many problems involving multicriteria decision making problems [13], medical diagnostics [14], pattern recognition [15] and mine safety [16] have all been solved extensively with neutrosophic differential equation.

A $\mathcal{N}_{number}$ is an extension of classical numbers and fuzzy numbers designed to handle uncertainty, indeterminacy, and vagueness more comprehensively. Parikh et al. [17] investigated logistic growth model that incorporates neutrosophic logic to better predict population dynamics, particularly when dealing with uncertainties and potential deviations. Bhaumik et al. [18] introduces a new ranking approach for handling uncertainty in game theory using single-valued triangular neutrosophic numbers by applying bi-matrix games. He demonstrated how neutrosophic logic can enhance decision-making processes in uncertain environments. Shanmugapriya et al. [19] explores a neutrosophic method to solve a system of first-order differential equations using Trapezoidal Neutrosophic Numbers. They incorporated $\left(\tilde{A},\tilde{B},\tilde{\Gamma}\right)_{cut}$, the approach accounts for varying levels of truth, indeterminacy, and falsity.

An important tool for understanding fluid flow dynamics under pressure gradients is the Falkner-Skan equation, which forms the basis of boundary layer theory. Its relevance and adaptability in the field of fluid dynamics are demonstrated by its applications in engineering design, theoretical analysis, numerical validation, and larger flow issues. Han [20] applied finite difference method for

finding numerical solution of Falkner-Skan wedge flow equation. Parand et al. [21] studied magnetohydrodynamics (MHD) Falkner-Skan wedge flow equation by leveraging the orthogonal Sinc functions to approximate solutions on semi-infinite domains with high accuracy. Elnady et al. [22] examined the solution of the Falkner–Skan equation by addressing the challenge of its semi-infinite domain. He tackled this by truncating the domain to a finite interval and then used a Chebyshev series to approximate the solution. Bararnia et al. [23] applied Homotopy Analysis Method (HAM) to solve the momentum and energy equation of Falkner-Skan wedge flow equation in incompressible fluid by using trial and error and Padé approximation. Shanmugapriya et al. [24, 25] and Gopi Krishna et al. [26] have studied fluid flow in wedge using various techniques.

Zulqarnain et al [27] employed a triangular fuzzy number to capture uncertainties and uses numerical methods to investigate how various parameters affect flow and heat transfer. He studied tri-hybrid nanofluid model incorporating Al_2O_3, Cu, TiO_2 in engine oil over a Riga wedge. Siddique et al [28] investigated the thermal properties of a second-grade hybrid nanofluid ($Al_2O_3 + Cu/EO$) over a Riga wedge, considering factors like heat source, stagnation point, and nonlinear thermal radiation in fuzzy environment. Shanmugapriya et al [29] explores the effects of endothermic/exothermic chemical reactions, thermal radiation, thermophoresis, and Brownian diffusion on the flow and heat transfer of a Casson hybrid nanofluid over a moving wedge under fuzzy environment.

1.1 Research gap

In the literature survey mentioned above, researchers have developed various methods to solve the Falkner-Skan equation, including similarity transformations, series solutions, and numerical methods like the finite difference method. However, but no research has addressed solutions using triangular and trapezoidal neutrosophic numbers. This research seeks to address this gap by examining neutrosophic solutions to the Falkner-Skan Boundary Layer Wedge flow equation through the application of both the shooting method and the Homotopy Perturbation Method (HPM).

1.2 Objective

The aim of this study is to investigate Falkner-Skan equation using $Tri\mathcal{N}_{number}$ and $Trap\mathcal{N}_{number}$. The ODE's are transformed into NDE's with the help of $\left(\widetilde{\mathrm{A}}, \widetilde{\mathrm{B}}, \widetilde{\Gamma}\right)_{cut}$. The $\mathcal{N}_{number}$ are applied in no slip conditions and wedge angle parameter. The shooting method via MATLAB and HPM via MAPLE were utilized to handle NDE's. The outcomes are validated through available literature, 2D and 3D plots.

1.3 Novelty

The novelty of the present study is

i. The behavior of Falkner-Skan wedge flow equation in neutrosophic environment has not been addressed previously.

ii. The wedge angle parameter $\tilde{\lambda}$ within the Falkner-Skan equation and no slip conditions are taken as $TriN_{number}$ and $TrapN_{number}$ through $(\widetilde{A}, \widetilde{B}, \widetilde{\Gamma})_{cut}$ approach covering a range of possible behavior.

iii. A comparative analysis of mean values and error profiles for $TriN_{number}$ and $TrapN_{number}$ are determined which highlights the performance in controlling uncertainty.

1.4 Applications

The use of trapezoidal and triangular neutrosophic numbers into the Falkner-Skan equation provides noteworthy benefits across several engineering domains through efficient uncertainty management:

i. Aerodynamics: By incorporating neutrosophic numbers into the design process, designers of automobiles and aircraft may better account for uncertainties in pressure gradients and flow conditions, resulting in more resilient and efficient designs that minimize drag and improve performance in ever changing situations.

ii. Industrial Heat Transfer: The use of neutrosophic numbers in heat exchangers and cooling systems makes designs more dependable and maintains efficiency in the face of temperature and flow rate variations, which is essential for energy-intensive businesses.

The above application shows how the Falkner-Skan equation's use of neutrosophic numbers improves fluid dynamics designs' performance and dependability by taking into account the inherent uncertainties of real-world scenarios.

The basic concepts of N_{set}, $(\widetilde{A}, \widetilde{B}, \widetilde{\Gamma})_{cut}$ of a N_{set}, N_{number}, $TriN_{number}$, $(\widetilde{A}, \widetilde{B}, \widetilde{\Gamma})_{cut}$ of $TriN_{number}$, $TrapN_{number}$, $(\widetilde{A}, \widetilde{B}, \widetilde{\Gamma})_{cut}$ of $TrapN_{number}$, and the $strong_{solution}$ of NDE are introduced in § 2.The mathematical formulation of Falkner-Skan equation is derived in § 3. In § 4, the equation is transmuted into neutrosophic equation and application of shooting method and HPM for neutrosophic governing equation. Finally, § 5 contains profile graphs, tables, neutrosophic analysis and comparative analysis of shooting method and HPM. The conclusion is given in § 6.

Abbreviation	**Description**
N_{set}	Neutrosophic Set
N_{number}	Neutrosophic Number
$(\widetilde{A}, \widetilde{B}, \widetilde{\Gamma})_{cut}$	$(\widetilde{A}, \widetilde{B}, \widetilde{\Gamma})$ cut
$TriN_{number}$	Triangular Neutrosophic Number
$(\widetilde{A}, \widetilde{B}, \widetilde{\Gamma})_{cut}$ of a $TriN_{number}$	$(\widetilde{A}, \widetilde{B}, \widetilde{\Gamma})$ cut of Triangular Neutrosophic Number

$Trap\mathcal{N}_{number}$	Trapezoidal Neutrosophic Number
$\left(\widetilde{\mathrm{A}},\widetilde{\mathrm{B}},\widetilde{\Gamma}\right)_{cut}$ of a $Trap\mathcal{N}_{number}$	$\left(\widetilde{\mathrm{A}},\widetilde{\mathrm{B}},\widetilde{\Gamma}\right)$ cut of Trapezoidal Neutrosophic Number
$strong_{solution}$	Strong Solution
$weak_{solution}$	Weak Solution
$truth_{function}$	Truth function
$indeterministic_{function}$	Indeterministic function
$falsity_{function}$	Falsity function
$Tri\mathcal{N}$ velocity	Triangular Neutrosophic Velocity
$Trap\mathcal{N}$ velocity	Trapezoidal Neutrosophic Velocity

2. Preliminaries

In this § 2, we recall a few preliminary concepts of neutrosophic set theory and some notations for better understanding.

Definition 2.1.

The universal set is typically denoted by X and is defined as the set of all objects or elements relevant to a discussion or problem.

Definition 2.2.[30]

Let X be a universe set. A $\mathcal{N}_{set}$ $\left(\widetilde{\mathcal{N}_s}\right)$ on X is defined as $\widetilde{\mathcal{N}_s} = \left\{\langle \mathcal{T}_{\widetilde{\mathcal{N}_s}}(x), \mathcal{I}_{\widetilde{\mathcal{N}_s}}(x), \mathcal{F}_{\widetilde{\mathcal{N}_s}}(x)\rangle : x \in X\right\}$, where $\mathcal{T}_{\widetilde{\mathcal{N}_s}}(x), \mathcal{I}_{\widetilde{\mathcal{N}_s}}(x), \mathcal{F}_{\widetilde{\mathcal{N}_s}}(x): X \to {}^{-}]0,1[^{+}$ represents the degree of certainty, degree of hesitation and degree of falseness respectively of the element $x \in X$ such that ${}^{-}0 \leq \mathcal{T}_{\widetilde{\mathcal{N}_s}}(x), +\mathcal{I}_{\widetilde{\mathcal{N}_s}}(x) + \mathcal{F}_{\widetilde{\mathcal{N}_s}}(x) \leq 3^{+}$.

Definition 2.3.[31]

The $\left(\widetilde{\mathrm{A}},\widetilde{\mathrm{B}},\widetilde{\Gamma}\right)_{cut}$ of $\mathcal{N}_{set}$ is defined as $\widetilde{\mathcal{N}_s}_{\left(\widetilde{\mathrm{A}},\widetilde{\mathrm{B}},\widetilde{\Gamma}\right)} = \left\{\langle \mathcal{T}_{\widetilde{\mathcal{N}_s}}(x), \mathcal{I}_{\widetilde{\mathcal{N}_s}}(x), \mathcal{F}_{\widetilde{\mathcal{N}_s}}(x)\rangle : x \in X, \mathcal{T}_{\widetilde{\mathcal{N}_s}}(x) \geq \widetilde{\mathrm{A}}, \mathcal{I}_{\widetilde{\mathcal{N}_s}}(x) \leq \widetilde{\mathrm{B}}, \mathcal{F}_{\widetilde{\mathcal{N}_s}}(x) \leq \widetilde{\Gamma}\right\}$, where $\widetilde{\mathrm{A}}, \widetilde{\mathrm{B}}, \widetilde{\Gamma} \in [0,1]$, such that $0 \leq \widetilde{\mathrm{A}} + \widetilde{\mathrm{B}} + \widetilde{\Gamma} \leq 3$.

Definition 2.4.[31]

A $\mathcal{N}_{set}$ defined on the set of real numbers $\mathbb{R}$ is a $\mathcal{N}_{number}$ if it satisfies the following properties:

i. $\widetilde{\mathcal{N}_s}$ is normal if $\exists\, x_0 \in \mathbb{R}: \mathcal{T}_{\widetilde{\mathcal{N}_s}}(x_0) = 1. \left(\mathcal{I}_{\widetilde{\mathcal{N}_s}}(x_0) = \mathcal{F}_{\widetilde{\mathcal{N}_s}}(x_0) = 0\right)$.

ii. $\widetilde{\mathcal{N}_s}$ is convex for the $truth_{function}$ $\mathcal{T}_{\widetilde{\mathcal{N}_s}}(x)$. $(ie)\mathcal{T}_{\widetilde{\mathcal{N}_s}}(\varsigma x_1 + (1-\varsigma)x_2) \geq \min\left(\mathcal{T}_{\widetilde{\mathcal{N}_s}}(x_1), \mathcal{T}_{\widetilde{\mathcal{N}_s}}(x_2)\right)$, for all $x_1, x_2 \in \mathbb{R}$ and $\varsigma \in [0,1]$.

iii. $\widetilde{\mathcal{N}_s}$ is concave set for the $indeterministic_{function}$ $\mathcal{I}_{\widetilde{\mathcal{N}_s}}(x)$ and $falsity_{function}$ $\mathcal{F}_{\widetilde{\mathcal{N}_s}}(x)$. $(ie)\ \mathcal{I}_{\widetilde{\mathcal{N}_s}}(\varsigma x_1 + (1-\varsigma)x_2) \geq \max\left(\mathcal{I}_{\widetilde{\mathcal{N}_s}}(x_1), \mathcal{I}_{\widetilde{\mathcal{N}_s}}(x_2)\right)$ and $(ie)\mathcal{F}_{\widetilde{\mathcal{N}_s}}(\varsigma x_1 + (1-\varsigma)x_2) \geq \max\left(\mathcal{F}_{\widetilde{\mathcal{N}_s}}(x_1), \mathcal{F}_{\widetilde{\mathcal{N}_s}}(x_2)\right)$, for all $x_1, x_2 \in \mathbb{R}$ and $\varsigma \in [0,1]$.

Definition 2.5.[31]

A $Tri\mathcal{N}_{number}$ is a subset of $\widetilde{\mathcal{N}_s}$ in $\mathbb{R}$ with the following $truth_{function}$, $indeterministic_{function}$, $falsity_{function}$ is defined as

$$\mathcal{T}_{\widetilde{\mathcal{N}_s}}(x) = \begin{cases} \left(\frac{x-a_1}{a_2-a_1}\right)\omega_{\widetilde{\mathcal{N}_s}} & if\ a_1 \le x \le a_2 \\ \omega_{\widetilde{\mathcal{N}_s}} & if\ x = a_2 \\ \left(\frac{a_3-x}{a_3-a_2}\right) & if\ a_2 \le x \le a_3 \\ 0 & otherwise \end{cases}$$

$$\mathcal{I}_{\widetilde{\mathcal{N}_s}}(x) = \begin{cases} \left(\frac{a_2-x}{a_2-a_1}\right)\delta_{\widetilde{\mathcal{N}_s}} & if\ a_1 \le x \le a_2 \\ \delta_{\widetilde{\mathcal{N}_s}} & if\ x = a_2 \\ \left(\frac{x-a_3}{a_3-a_2}\right) & if\ a_2 \le x \le a_3 \\ 1 & otherwise \end{cases} \quad (2.1)$$

$$\mathcal{F}_{\widetilde{\mathcal{N}_s}}(x) = \begin{cases} \left(\frac{a_2-x}{a_2-a_1}\right)\varepsilon_{\widetilde{\mathcal{N}_s}} & if\ a_1 \le x \le a_2 \\ \varepsilon_{\widetilde{\mathcal{N}_s}} & if\ x = a_2 \\ \left(\frac{x-a_3}{a_3-a_2}\right) & if\ a_2 \le x \le a_3 \\ 1 & otherwise \end{cases}$$

where $^-0 \le \mathcal{T}_{\widetilde{\mathcal{N}_s}}(x) + \mathcal{I}_{\widetilde{\mathcal{N}_s}}(x) + \mathcal{F}_{\widetilde{\mathcal{N}_s}}(x) \le 3^+, x \in \widetilde{\mathcal{N}_s}$.

Definition 2.6.[31]

The $\left(\widetilde{\mathrm{A}}, \widetilde{\mathrm{B}}, \widetilde{\Gamma}\right)_{cut}$ of a $Tri\mathcal{N}_{number} = \langle (a_1, a_2, a_3); \omega_{\widetilde{\mathcal{N}_s}}, \delta_{\widetilde{\mathcal{N}_s}}, \varepsilon_{\widetilde{\mathcal{N}_s}} \rangle$ is defined as follows:

$\widetilde{\mathcal{N}_s}_{(\widetilde{\mathrm{A}},\widetilde{\mathrm{B}},\widetilde{\Gamma})} = \left[\mathcal{T}_{\widetilde{\mathcal{N}_s}^1}(\widetilde{\mathrm{A}}), \mathcal{T}_{\widetilde{\mathcal{N}_s}^2}(\widetilde{\mathrm{A}}); \mathcal{I}_{\widetilde{\mathcal{N}_s}^1}(\widetilde{\mathrm{B}}), \mathcal{I}_{\widetilde{\mathcal{N}_s}^2}(\widetilde{\mathrm{B}}); \mathcal{F}_{\widetilde{\mathcal{N}_s}^1}(\widetilde{\Gamma}), \mathcal{F}_{\widetilde{\mathcal{N}_s}^2}(\widetilde{\Gamma})\right]$, where

$$\begin{aligned} &\mathcal{T}_{\widetilde{\mathcal{N}_s}^1}(\widetilde{\mathrm{A}}) = \left[a_1 + \widetilde{\mathrm{A}}(a_2 - a_1)\right]\omega_{\widetilde{\mathcal{N}_s}}, \mathcal{T}_{\widetilde{\mathcal{N}_s}^2}(\widetilde{\mathrm{A}}) = \left[a_3 - \widetilde{\mathrm{A}}(a_3 - a_2)\right]\omega_{\widetilde{\mathcal{N}_s}} \\ &\mathcal{I}_{\widetilde{\mathcal{N}_s}^1}(\widetilde{\mathrm{A}}) = \left[a_2 - \widetilde{\mathrm{B}}(a_2 - a_1)\right]\delta_{\widetilde{\mathcal{N}_s}}, \mathcal{I}_{\widetilde{\mathcal{N}_s}^2}(\widetilde{\mathrm{A}}) = \left[a_2 + \widetilde{\mathrm{B}}(a_3 - a_2)\right]\delta_{\widetilde{\mathcal{N}_s}} \\ &\mathcal{F}_{\widetilde{\mathcal{N}_s}^1}(\widetilde{\mathrm{A}}) = \left[a_2 - \widetilde{\Gamma}(a_2 - a_1)\right]\varepsilon_{\widetilde{\mathcal{N}_s}}, \mathcal{F}_{\widetilde{\mathcal{N}_s}^2}(\widetilde{\mathrm{A}}) = \left[a_2 + \widetilde{\Gamma}(a_3 - a_2)\right]\varepsilon_{\widetilde{\mathcal{N}_s}} \end{aligned} \quad (2.2)$$

Here $0 \le \widetilde{\mathrm{A}} \le 1, 0 \le \widetilde{\mathrm{B}} \le 1, 0 \le \widetilde{\Gamma} \le 1$ and $^-0 \le \widetilde{\mathrm{A}} + \widetilde{\mathrm{B}} + \widetilde{\Gamma} \le 3^+$ and is displayed in Figure 1.

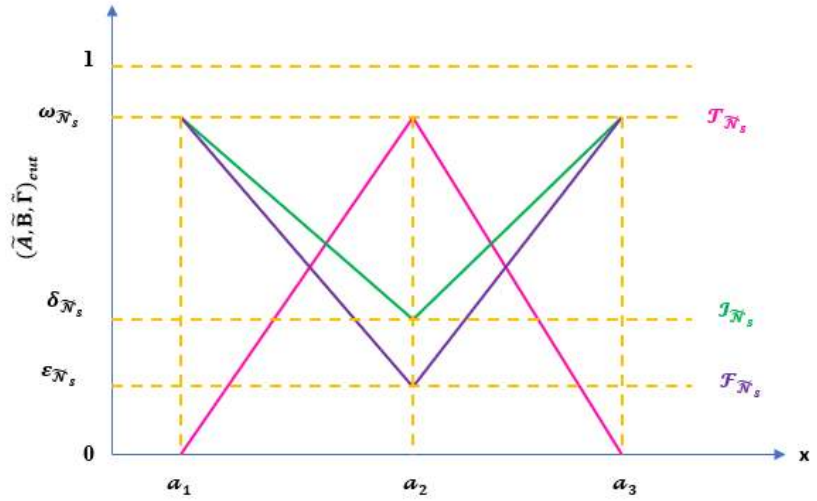

Figure 1. Membership function of $Tri\mathcal{N}_{number}$

Definition 2.7.[32]

A $Trap\mathcal{N}_{number}$ is a subset of $\widetilde{\mathcal{N}_s}$ in $\mathbb{R}$ with the following $truth_{function}$, $indeterministic_{function}$, $falsity_{function}$ is defined as

$$\mathcal{T}_{\widetilde{\mathcal{N}_s}}(x)=\begin{cases}\left(\frac{x-a_1}{a_2-a_1}\right)\omega_{\widetilde{\mathcal{N}_s}} & if\ a_1\le x\le a_2\\ \omega_{\widetilde{\mathcal{N}_s}} & if\ a_2\le x\le a_3\\ \left(\frac{a_4-x}{a_4-a_3}\right) & if\ a_3\le x\le a_4\\ 0 & otherwise\end{cases}$$

$$\mathcal{I}_{\widetilde{\mathcal{N}_s}}(x)=\begin{cases}\left(\frac{a_2-x}{a_2-a_1}\right)\delta_{\widetilde{\mathcal{N}_s}} & if\ a_1\le x\le a_2\\ \delta_{\widetilde{\mathcal{N}_s}} & if\ a_2\le x\le a_3\\ \left(\frac{a_4-x}{a_4-a_3}\right) & if\ a_3\le x\le a_4\\ 1 & otherwise\end{cases} \tag{2.3}$$

$$\mathcal{F}_{\widetilde{\mathcal{N}_s}}(x)=\begin{cases}\left(\frac{a_2-x}{a_2-a_1}\right)\varepsilon_{\widetilde{\mathcal{N}_s}} & if\ a_1\le x\le a_2\\ \varepsilon_{\widetilde{\mathcal{N}_s}} & if\ a_2\le x\le a_3\\ \left(\frac{a_4-x}{a_4-a_3}\right) & if\ a_3\le x\le a_4\\ 1 & otherwise\end{cases}$$

where $^-0\le\mathcal{T}_{\widetilde{\mathcal{N}_s}}(x)+\mathcal{I}_{\widetilde{\mathcal{N}_s}}(x)+\mathcal{F}_{\widetilde{\mathcal{N}_s}}(x)\le 3^+, x\in\widetilde{\mathcal{N}_s}$.

Definition 2.8.[32]

The $\left(\widetilde{\mathrm{A}},\widetilde{\mathrm{B}},\widetilde{\Gamma}\right)_{cut}$ of a $Trap\mathcal{N}_{number}=\langle(a_1,a_2,a_3,a_4);\omega_{\widetilde{\mathcal{N}_s}},\delta_{\widetilde{\mathcal{N}_s}},\varepsilon_{\widetilde{\mathcal{N}_s}}\rangle$ is defined as follows:

$\widetilde{\mathcal{N}_s}_{(\widetilde{\mathrm{A}},\widetilde{\mathrm{B}},\widetilde{\Gamma})}=\left[\mathcal{T}_{\widetilde{\mathcal{N}_{s^1}}}(\widetilde{\mathrm{A}}),\mathcal{T}_{\widetilde{\mathcal{N}_{s^2}}}(\widetilde{\mathrm{A}});\mathcal{I}_{\widetilde{\mathcal{N}_{s^1}}}(\widetilde{\mathrm{B}}),\mathcal{I}_{\widetilde{\mathcal{N}_{s^2}}}(\widetilde{\mathrm{B}});\mathcal{F}_{\widetilde{\mathcal{N}_{s^1}}}(\widetilde{\Gamma}),\mathcal{F}_{\widetilde{\mathcal{N}_{s^2}}}(\widetilde{\Gamma})\right]$, where

$$\begin{aligned}&\mathcal{T}_{\widetilde{\mathcal{N}_{s^1}}}(\widetilde{\mathrm{A}})=\left[a_1+\widetilde{\mathrm{A}}(a_2-a_1)\right]\omega_{\widetilde{\mathcal{N}_s}},\ \mathcal{T}_{\widetilde{\mathcal{N}_{s^2}}}(\widetilde{\mathrm{A}})=\left[a_4-\widetilde{\mathrm{A}}(a_4-a_3)\right]\omega_{\widetilde{\mathcal{N}_s}}\\ &\mathcal{I}_{\widetilde{\mathcal{N}_{s^1}}}(\widetilde{\mathrm{A}})=\left[a_2-\widetilde{\mathrm{B}}(a_2-a_1)\right]\delta_{\widetilde{\mathcal{N}_s}},\ \mathcal{I}_{\widetilde{\mathcal{N}_{s^2}}}(\widetilde{\mathrm{A}})=\left[a_3+\widetilde{\mathrm{B}}(a_4-a_3)\right]\delta_{\widetilde{\mathcal{N}_s}}\\ &\mathcal{F}_{\widetilde{\mathcal{N}_{s^1}}}(\widetilde{\mathrm{A}})=\left[a_2-\widetilde{\Gamma}(a_2-a_1)\right]\varepsilon_{\widetilde{\mathcal{N}_s}},\ \mathcal{F}_{\widetilde{\mathcal{N}_{s^2}}}(\widetilde{\mathrm{A}})=\left[a_3+\widetilde{\Gamma}(a_4-a_3)\right]\varepsilon_{\widetilde{\mathcal{N}_s}}\end{aligned} \tag{2.4}$$

Here $0\le\widetilde{\mathrm{A}}\le 1, 0\le\widetilde{\mathrm{B}}\le 1, 0\le\widetilde{\Gamma}\le 1$ and $^-0\le\widetilde{\mathrm{A}}+\widetilde{\mathrm{B}}+\widetilde{\Gamma}\le 3^+$ and is displayed in Figure 2.

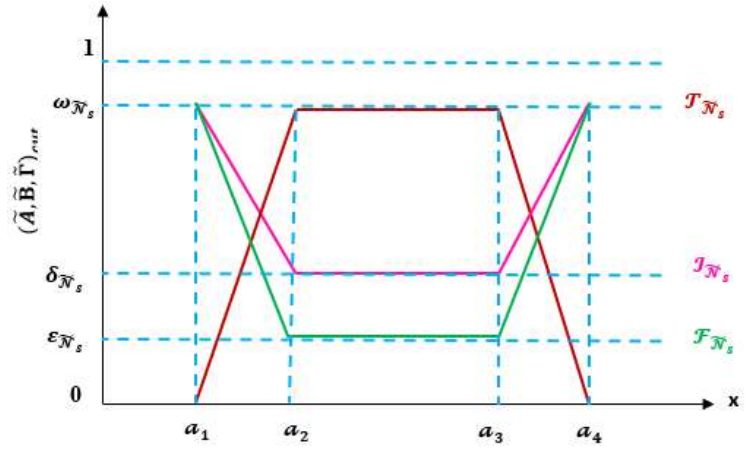

Figure 2. Membership function of $Trap\mathcal{N}_{number}$

Definition 2.9.[32] Let the solution of the neutrosophic differential equation be $y(x)$ and its $(\tilde{A},\tilde{B},\tilde{\Gamma})_{cut}$ be $[y(x,\tilde{A},\tilde{B},\tilde{\Gamma})] = \left[\left(y_1(x,\tilde{A}), y_2(x,\tilde{A}), y_1'(x,\tilde{B}), y_2'(x,\tilde{B}), y_1''(x,\tilde{\Gamma}), y_2''(x,\tilde{\Gamma})\right)\right]$. The solution is a $strong_{solution}$

$$\begin{aligned}
&i. \quad \frac{dy_1(x,\tilde{A})}{d\tilde{A}} > 0, \frac{dy_2(x,\tilde{A})}{d\tilde{A}} < 0, \forall\, \tilde{A} \in [0,1], y_1(x,1) \le y_2(x,1).\\
&ii. \quad \frac{dy_1'(x,\tilde{B})}{d\tilde{B}} < 0, \frac{dy_2'(x,\tilde{B})}{d\tilde{B}} > 0, \forall\, \tilde{B} \in [0,1], y_1'(x,0) \le y_2'(x,0). \qquad (2.5)\\
&iii. \quad \frac{dy_1''(x,\tilde{\Gamma})}{d\tilde{\Gamma}} < 0, \frac{dy_2''(x,\tilde{\Gamma})}{d\tilde{\Gamma}} > 0, \forall\, \tilde{\Gamma} \in [0,1], y_1''(x,0) \le y_2''(x,0).
\end{aligned}$$

Otherwise the solution is $week_{solution}$.

3. Falkner-Skan Equation

The Falkner-Skan equation is a third-order nonlinear ordinary differential equation (ODE) that arises in the study of boundary layer flows over a wedge. Named after V.M. Falkner and S.W. Skan, this equation generalizes the Blasius equation for boundary layer flows over a flat plate to include the effects of a pressure gradient. The governing equation is derived from the boundary layer equations, which are simplifications of the Navier-Stokes equations for high Reynolds number flows where viscous effects are confined to thin regions near solid boundaries. The solution to the Falkner–Skan equation is significant in fluid dynamics as it describes the behavior of the laminar boundary layer over an infinite wedge. The wedge has a vertex angle of $\tilde{\lambda}\pi$, where $0 \le \tilde{\lambda} \le 2$.The parameter $\tilde{\lambda}$ controls the shape and flow characteristics of the boundary layer. The range $0 \le \tilde{\lambda} \le 2$ indicates different flow regimes: 1) $\tilde{\lambda} = 0$ represents the boundary layer over a flat plate (Blasius solution). 2) $0 < \tilde{\lambda} < 1$ describes accelerating flows, where the flow speed increases as it moves along the surface. 3) $\tilde{\lambda} = 1$:

Represents a stagnation point flow, where the fluid approaches the surface perpendicularly. 4) $1 < \tilde{\lambda} \leq 2$: Describes decelerating flows, where the flow speed decreases along the surface.

For a steady, incompressible, two-dimensional boundary layer flow over a wedge, the boundary layer equations in Cartesian coordinates (x, y) are: [33]

$$\frac{\partial u}{\partial x} + \frac{\partial v}{\partial y} = 0 \tag{3.1}$$

$$u\frac{\partial u}{\partial x} + v\frac{\partial v}{\partial y} = U\frac{dU}{dx} + \varpi\frac{\partial^2 u}{\partial y^2} \tag{3.2}$$

with boundary conditions

$$u = 0, v = 0 \; at \; y = 0 \text{ and } u(x, y) = U(x) \; as \; y \to \infty. \tag{3.3}$$

Here $u$and v are the velocity components in the x and y directions, respectively. U is the external velocity at the edge of the boundary layer. ϖ is the kinematic viscosity of the fluid.

3.1 Similarity Transformation

To simplify these equations, we introduce a similarity variable ζ and a stream function χ defined as: [34]

$$\zeta = y\sqrt{\frac{c(m+1)}{2\varpi_f}x^{m-1}}\;, \chi(x, y) = \left[\frac{2c\varpi_f}{m+1}x^{m+1}\right]^{0.5} f(\zeta) \tag{3.4}$$

where $f(\zeta)$ is the dimensionless stream function. The velocity components can be expressed in terms of $f(\zeta)$ as:

$$u = \frac{\partial \chi}{\partial y} = cx^m f'(\zeta), v = \frac{-\partial \chi}{\partial x} = \left[\frac{-\varpi_f c x^{m-1}(m+1)}{2}\right]^{0.5}\left[\zeta f'(\zeta)\frac{(m-1)}{(m+1)} + f(\zeta)\right] \tag{3.5}$$

Substituting these into the boundary layer equations and simplifying, we obtain the Falkner-Skan equation:

$$f''' + ff' + \tilde{\lambda}[1 - (f')^2] = 0 \tag{3.6}$$

where $\tilde{\lambda}$ is the Falkner-Skan parameter related to the pressure gradient and is defines as: $\tilde{\lambda} = \frac{2m}{m+1}$.

Here, m is related to the external velocity $U(x)$ as $U(x) \propto x^m$.

The boundary conditions for the Falkner-Skan equation are:

$$\left.\begin{matrix} f(\zeta) = 0,\; f'(\zeta) = 0 & as\; \zeta \to 0 \\ f'(\zeta) \to 1 & as\; \zeta \to \infty \end{matrix}\right\} \tag{3.7}$$

These conditions correspond to the no-slip condition at the wall and the matching of the velocity to the external flow far from the wall.

The Falkner-Skan equation is used to analyze the effects of pressure gradients on boundary layer flows. Positive $\tilde{\lambda}$ (or $m > 0$) corresponds to a favorable pressure gradient (accelerating flow), while negative $\tilde{\lambda}$ (or $m < 0$) corresponds to an adverse pressure gradient (decelerating flow).

4. Methodology

4.1 Application of numerical technique

We can use the shooting method to solve boundary value problem (BVP) by converting them into initial value problem (IVP). By transforming the third-order ODE into a first-order ODE and solved using MATLAB's numerical solvers. The shooting method involves guessing the initial conditions for the IVP at $\zeta = 0$, integrating the first-order ODE, and adjusting the guessed initial conditions to satisfy the boundary conditions at the other endpoint (as $\zeta \to \infty$). The tolerance level in the case of the present problem is 10^{-6}. It is highly sensitive to initial guesses for the unknown initial conditions, and poor choices can be to diverges or incorrect solutions. This method may not always converge particularly for highly nonlinear coupled equations. These challenges make this method to less reliable in certain situation.

Let $f = i_1, f' = i_2, f'' = i_3$.

Then the system of equations becomes

$$\begin{bmatrix} i_1' \\ i_2' \\ i_3' \end{bmatrix} = \begin{bmatrix} i_2 \\ i_3 \\ -i_1 i_3 - \tilde{\lambda}[1 - (i_2)^2] \end{bmatrix} \tag{4.1}$$

along with boundary conditions

$$i_1(\zeta) = i_2(\zeta) = 0, \ \ as\ \zeta \to\ 0 \text{ and } i_2(\zeta) = 1\ as\ \zeta \to \infty \tag{4.2}$$

4.1.1 Formulation of Falkner-Skan Equation in Neutrosophic Environment

In the neutrosophic context, the function $f(\zeta)$ and its derivatives will have three components each: $\widetilde{\mathrm{A}}$ (truth), $\widetilde{\mathrm{B}}$ (indeterminacy), and $\tilde{\Gamma}$ (falsity). Denote these as:

$$f(\zeta) = \left(f(\zeta, \widetilde{\mathrm{A}}), f(\zeta, \widetilde{\mathrm{B}}), f(\zeta, \tilde{\Gamma})\right) \tag{4.3}$$

This means that for the function $f(\zeta)$ its derivatives, and the constants, we will consider three corresponding components. The neutrosophic form of the Falkner-Skan equation can then be written as a set of three coupled differential equations:

$$\left.\begin{aligned} f'''(\zeta, \widetilde{\mathrm{A}}) + f(\zeta, \widetilde{\mathrm{A}}) f'(\zeta, \widetilde{\mathrm{A}}) + \tilde{\lambda}^{\widetilde{\mathrm{A}}}\left[1 - \left(f'(\zeta, \widetilde{\mathrm{A}})\right)^2\right] = 0 \\ f'''(\zeta, \widetilde{\mathrm{B}}) + f(\zeta, \widetilde{\mathrm{B}}) f'(\zeta, \widetilde{\mathrm{B}}) + \tilde{\lambda}^{\widetilde{\mathrm{B}}}\left[1 - \left(f'(\zeta, \widetilde{\mathrm{B}})\right)^2\right] = 0 \\ f'''(\zeta, \tilde{\Gamma}) + f(\zeta, \tilde{\Gamma}) f'(\zeta, \tilde{\Gamma}) + \tilde{\lambda}^{\tilde{\Gamma}}\left[1 - \left(f'(\zeta, \tilde{\Gamma})\right)^2\right] = 0 \end{aligned}\right\} \tag{4.4}$$

with the transformed boundary condition

$$\left.\begin{array}{l} f(\zeta,\widetilde{\mathrm{A}})=\tilde{0},\ f'(\zeta,\widetilde{\mathrm{A}})=\tilde{0}\ as\ \zeta\to\ 0\ ,\ f'(\zeta,\widetilde{\mathrm{A}})\to 1\ as\ \zeta\to\infty \\ f(\zeta,\widetilde{\mathrm{B}})=\tilde{0},\ f'(\zeta,\widetilde{\mathrm{B}})=\tilde{0} as\ \zeta\to\ 0\ ,\ f'(\zeta,\widetilde{\mathrm{B}})\to 1\ as\ \zeta\to\infty \\ f(\zeta,\tilde{\Gamma})=\tilde{0},\ f'(\zeta,\tilde{\Gamma})=\tilde{0}\ as\ \zeta\to\ 0\ ,\ f'(\zeta,\tilde{\Gamma})\to 1\ as\ \zeta\to\infty \end{array}\right\} \quad (4.5)$$

where the neutrosophic velocity profile $f'(\zeta,\widetilde{\mathrm{A}})=\left[\underline{\mathrm{f}'}(\zeta,\widetilde{\mathrm{A}}),\overline{\mathrm{f}'}(\zeta,\widetilde{\mathrm{A}})\right], 0\le\widetilde{\mathrm{A}}\le 1$. The term $\underline{\mathrm{f}'}(\zeta,\widetilde{\mathrm{A}})$ and $\overline{\mathrm{f}'}(\zeta,\widetilde{\mathrm{A}})$ represents the lower and upper bounds of the neutrosophic velocity, respectively for $\widetilde{\mathrm{A}}$ (truth). Similarly, $f'(\zeta,\widetilde{\mathrm{B}})=\left[\underline{\mathrm{f}'}(\zeta,\widetilde{\mathrm{B}}),\overline{\mathrm{f}'}(\zeta,\widetilde{\mathrm{B}})\right]$, $f'(\zeta,\tilde{\Gamma})=\left[\underline{\mathrm{f}'}(\zeta,\tilde{\Gamma}),\overline{\mathrm{f}'}(\zeta,\tilde{\Gamma})\right], 0\le\widetilde{\mathrm{B}}\le 1, 0\le\tilde{\Gamma}\le 1$ for $\widetilde{\mathrm{B}}$ (indeterminacy) and $\tilde{\Gamma}$ (falsity), respectively and $^{-}0\le\widetilde{\mathrm{A}}+\widetilde{\mathrm{B}}+\tilde{\Gamma}\le 3^{+}$.

4.2 Application of semi-analytic technique

The basic concept of the HPM to a non-linear differential equation is

$$R(C)-s(\widetilde{\Lambda})=0,\qquad \widetilde{\Lambda}\in\Omega \quad (4.6)$$

The corresponding boundary conditions are

$$Z\left(C,\frac{\partial C}{\partial n}\right)=0\ ,\widetilde{\Lambda}\in\Gamma \quad (4.7)$$

where R is a general non-linear differential operator, B is a boundary operator, $s(\widetilde{\Lambda})$ a known analytical function and $\widetilde{\Lambda}$ the boundary of domain Ω.

The operator R can be divided into two namely L and N, where L is the linear operator, while N is a non-linear operator of Eq. (4.6) which can be written as:

$$L(C)+N(C)-s(\widetilde{\Lambda})=0,\widetilde{\Lambda}\in\Omega \quad (4.8)$$

Define a homotopy as follows:

$$\mathcal{H}(f,\xi)=(1-\xi)[L(f)]+\xi[N(f)]=0, \quad (4.9)$$

where $\xi=[0,1]$ is an embedding parameter.

Its accuracy depends on the initial approximation, and poor choices may lead to inaccurate solutions. This method may also produce dual solutions, depending on how the homotopy id constructed, creating ambiguity in selecting the correct one. Moreover, it doesn't guarantee convergence highly nonlinear coupled equations.

For Falkner-Skan equation, $L(f)=f'''$ and $N(f)=f'''+ff'+\tilde{\lambda}[1-(f')^2]$. Now construct the homotopy as:

$$(1-\xi)f'''+\xi\left[f'''+ff'+\tilde{\lambda}[1-(f')^2]\right]=0 \quad (4.10)$$

Assume a solution in the form of a power series in ξ:

$$f=f_0+\xi f_1+\xi^2 f_2+\cdots=\sum_{j=1}^{n}\xi^j f_j \quad (4.11)$$

Substituting Eq. (4.11) into Eq. (4.10), we get the co-efficient of different powers of ξ:

$$\xi^0: f_0'''=0 \quad (4.12)$$

$$f_0(0)=f_0'(0)=0\ ,f_0'(\infty)=1$$

$$\xi^1: f_1'''=-f_0f_0''-\tilde{\lambda}[1-(f_0')^2] \quad (4.13)$$

$f_1(0) = f_1'(0) = 0\,, f_1'(\infty) = 0$

$\xi^2 : f_2''' = -f_0 f_1'' - f_0'' f_1 + 2\tilde{\lambda} f_0' f_1'$ (4.14)

$f_2(0) = f_2'(0) = 0\,, f_2'(\infty) = 0$

Solving (4.12), (4.13) and (4.14), we have

$$\left.\begin{aligned} f_0(\zeta) &= \frac{\zeta^2}{2\zeta_\infty} \\ f_1(\zeta) &= -\frac{k}{60}\zeta^5 - \frac{\tilde{\lambda}}{6}\zeta^3 \\ f_2(\zeta) &= \frac{\left[\left(\frac{(1-\tilde{\lambda})k + (k/10)}{1764}\right)\zeta^8 + \left(\frac{(2\tilde{\lambda}/3) - \tilde{\lambda}^2}{120}\right)\zeta^6\right]}{\zeta_\infty} \end{aligned}\right\} \quad (4.15)$$

4.2.1 Formulation of Falkner-Skan Equation in Neutrosophic Environment

We introduce a neutrosophic approach to solve uncertainty parameter $\tilde{\lambda}$ and boundary condition, using $TriN_{number}$ and $TrapN_{number}$. Our methodology involves applying $\left(\widetilde{A}, \widetilde{B}, \tilde{\Gamma}\right)_{cut}$ to represent various degrees of truth, indeterminacy, and falsity. We developed a solution procedure that integrates these neutrosophic numbers into HPM.

$$\left.\begin{aligned} (1-\zeta)\, f'''(\zeta, \widetilde{A}) + \zeta\left[f'''(\zeta, \widetilde{A}) + f(\zeta, \widetilde{A}) f'(\zeta, \widetilde{A}) + \tilde{\lambda}^{\widetilde{A}}\left[1 - \left(f'(\zeta, \widetilde{A})\right)^2\right]\right] = 0 \\ (1-\zeta) f'''(\zeta, \widetilde{B}) + \zeta\left[f'''(\zeta, \widetilde{B}) + f(\zeta, \widetilde{B}) f'(\zeta, \widetilde{B}) + \tilde{\lambda}^{\widetilde{B}}\left[1 - \left(f'(\zeta, \widetilde{B})\right)^2\right]\right] = 0 \\ (1-\zeta) f'''(\zeta, \tilde{\Gamma}) + \zeta\left[f'''(\zeta, \tilde{\Gamma}) + f(\zeta, \tilde{\Gamma}) f'(\zeta, \tilde{\Gamma}) + \tilde{\lambda}^{\tilde{\Gamma}}\left[1 - \left(f'(\zeta, \tilde{\Gamma})\right)^2\right]\right] = 0 \end{aligned}\right\} \quad (4.16)$$

with the transformed boundary condition

$$\left.\begin{aligned} f(\zeta, \widetilde{A}) = \tilde{0},\ f'(\zeta, \widetilde{A}) = \tilde{0}\ as\ \zeta \to 0\ ,\ f'(\zeta, \widetilde{A}) \to 1\ as\ \zeta \to \infty \\ f(\zeta, \widetilde{B}) = \tilde{0},\ f'(\zeta, \widetilde{B}) = \tilde{0}\ as\ \zeta \to 0\ ,\ f'(\zeta, \widetilde{B}) \to 1\ as\ \zeta \to \infty \\ f(\zeta, \tilde{\Gamma}) = \tilde{0},\ f'(\zeta, \tilde{\Gamma}) = \tilde{0}\ as\ \zeta \to 0\ ,\ f'(\zeta, \tilde{\Gamma}) \to 1\ as\ \zeta \to \infty \end{aligned}\right\} \quad (4.17)$$

where the neutrosophic velocity profile $f'(\zeta, \widetilde{A}) = \left[\underline{f'}(\zeta, \widetilde{A}), \overline{f'}(\zeta, \widetilde{A})\right], 0 \le \widetilde{A} \le 1$. The term $\underline{f'}(\zeta, \widetilde{A})$ and $\overline{f'}(\zeta, \widetilde{A})$ represents the lower and upper bounds of the neutrosophic velocity, respectively for $\widetilde{A}$ (truth). Similarly, $f'(\zeta, \widetilde{B}) = \left[\underline{f'}(\zeta, \widetilde{B}), \overline{f'}(\zeta, \widetilde{B})\right]$, $f'(\zeta, \tilde{\Gamma}) = \left[\underline{f'}(\zeta, \tilde{\Gamma}), \overline{f'}(\zeta, \tilde{\Gamma})\right], 0 \le \widetilde{B} \le 1, 0 \le \tilde{\Gamma} \le 1$ for $\widetilde{B}$ (indeterminacy) and $\tilde{\Gamma}$ (falsity), respectively and $^{-}0 \le \widetilde{A} + \widetilde{B} + \tilde{\Gamma} \le 3^{+}$.

The $TriN_{number}$ and $TriN_{number}$ are transformed using $\left(\widetilde{A}, \widetilde{B}, \tilde{\Gamma}\right)_{cut}$ technique shown in Table 1 and 2.

	Crisp value	$\mathcal{N}_{number}$	**Alpha cut approach**	**Beta cut approach**	**Gamma cut approach**
$\boldsymbol{TriN_{number}}$	[0.01-0.4]	[0.2,0.4,0.6;0.7,0.3,0.5]	[(0.2+0.2$\widetilde{A}$)0.7, (0.6 – 0.2$\widetilde{A}$)0.7]	[(0.4-0.2$\widetilde{B}$)0.3, (0.4 + 0.2$\widetilde{B}$)0.3]	[(0.4-0.2$\tilde{\Gamma}$)0.5, (0.4 + 0.2$\tilde{\Gamma}$)0.5]

$\boldsymbol{TrapN_{number}}$	[0.01-0.4]	[0.2,0.4,0.6,0.8;0.7,0.3,0.5]	[(0.2+0.2$\widetilde{A}$)0.7, (0.8 – 0.2$\widetilde{A}$)0.7]	[(0.4-0.2$\widetilde{B}$)0.3, (0.6 + 0.2$\widetilde{B}$)0.3]	[(0.4-0.2$\widetilde{\Gamma}$)0.5, (0.6 + 0.2$\widetilde{\Gamma}$)0.5]

Table 1. Parametric form of $TriN_{number}$ and $TrapN_{number}$ for wedge angle parameter $\tilde{\lambda}$

Table 2. Parametric form of $TriN_{number}$ and $TrapN_{number}$ for no slip conditions

	No slip Conditions	**Crisp value**	$\boldsymbol{N_{number}}$	**Alpha cut approach**	**Beta cut approach**	**Gamma cut approach**
$\boldsymbol{TriN_{number}}$	$f(\zeta) = \tilde{0}$,	[0.01-0.4]	[0.1,0.3,0.5; 0.6,0.4,0.2]	[(0.1+0.2$\widetilde{A}$)0.6, (0.5 – 0.2$\widetilde{A}$)0.6]	[(0.3-0.2$\widetilde{B}$)0.4, (0.3 + 0.2$\widetilde{B}$)0.4]	[(0.3-0.2$\widetilde{\Gamma}$)0.2, (0.3 + 0.2$\widetilde{\Gamma}$)0.2]
	$f'(\zeta) = \tilde{0}$	[0.01-0.4]	[0.2,0.4,0.6; 0.7,0.3,0.5]	[(0.2+0.2$\widetilde{A}$)0.7, (0.6 – 0.2$\widetilde{A}$)0.7]	[(0.4-0.2$\widetilde{B}$)0.3, (0.4 + 0.2$\widetilde{B}$)0.3]	[(0.4-0.2$\widetilde{\Gamma}$)0.5, (0.4 + 0.2$\widetilde{\Gamma}$)0.5]
$\boldsymbol{TrapN_{number}}$	$f(\zeta) = \tilde{0}$	[0.01-0.4]	[0.1,0.3,0.5,0.7; 0.6,0.4,0.2]	[(0.1+0.2$\widetilde{A}$)0.6, (0.7 – 0.2$\widetilde{A}$)0.6]	[(0.3-0.2$\widetilde{B}$)0.4, (0.5 + 0.2$\widetilde{B}$)0.4]	[(0.3-0.2$\widetilde{\Gamma}$)0.2, (0.5+ 0.2$\widetilde{\Gamma}$)0.2]
	$f'(\zeta) = \tilde{0}$	[0.01-0.4]	[0.2,0.4,0.6,0.8; 0.7,0.3,0.5]	[(0.2+0.2$\widetilde{A}$)0.7, (0.8 – 0.2$\widetilde{A}$)0.7]	[(0.4-0.2$\widetilde{B}$)0.3, (0.6 + 0.2$\widetilde{B}$)0.3]	[(0.4-0.2$\widetilde{\Gamma}$)0.5, (0.6 + 0.2$\widetilde{\Gamma}$)0.5]

4.3 Validation

To check the accuracy of the numerical and semi-analytic scheme, the results of $f''(0)$ of Falkner-Skan equation was compared with Zhang et al. [35] and Salama [36].

Table 3. Comparison of $f''(0)$ for various values of $\tilde{\lambda}$

$\tilde{\lambda}$	**Zhang et al. [35]**	**Salama [36]**	**Present (Shooting method)**	**Present (HPM)**
-0.15	0.216362	0.216362	0.216362	0.288217
-0.1	0.319270	0.319270	0.319269	0.359690
0	0.469600	0.469600	0.469599	0.493155
0.5	0.927680	0.927680	0.927680	0.970833
1	1.232587	1.232588	1.232587	1.132440

5. Result and discussion

In this section, we concentrated on the neutrosophic analysis of Falkner-Skan equation. The uncertainty of wedge angle parameter $\tilde{\lambda}$ and no slip conditions are considered as $TriN_{number}$ and $TrapN_{number}$. The governing equation is transformed as a NDE's, are numerically solved using the shooting method and HPM. The solution process involves application of the $(\widetilde{A}, \widetilde{B}, \widetilde{\Gamma})_{cut}$ techniques.

5.1 Profile graph of Falkner-Skan Equation via Shooting Method

Figure 3 illustrates that the velocity distribution within the boundary layer increases as $\tilde{\lambda}$ is augmented. The observed trends show that controlling the wedge angle parameter $\tilde{\lambda}$ is an effective

strategy to modulate boundary layer characteristics, particularly in applications requiring specific flow acceleration.

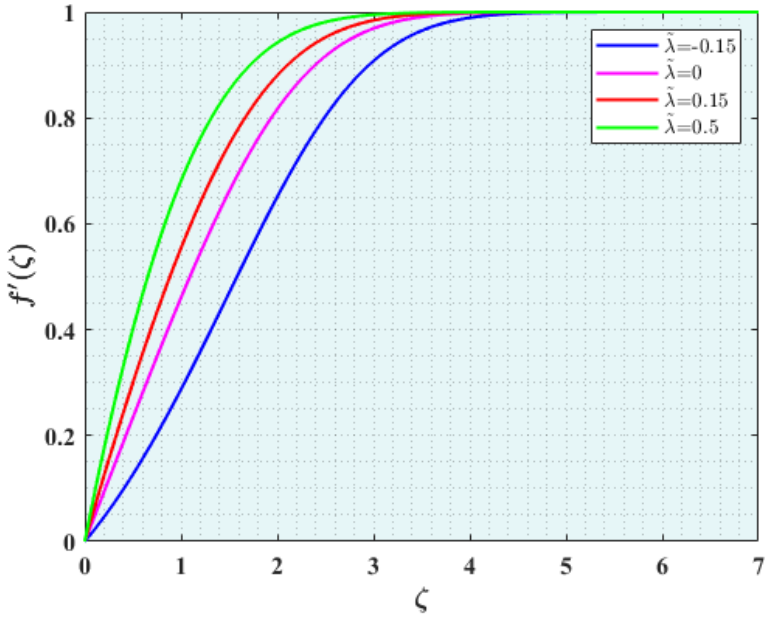

Figure 3. Behavior of $f'(\zeta)$ against $\tilde{\lambda}$

5.1.1 Neutrosophic Analysis using shooting method

Case 1: No slip condition as $\mathcal{N}_{number}$

The no slip conditions are taken as $Tri\mathcal{N}_{number}$ and $Trap\mathcal{N}_{number}$. From Figure 4 and 5, we see that $\underline{f'}(\zeta, \tilde{A})$ is increasing and $\overline{f'}(\zeta, \tilde{A})$ is decreasing for all $\tilde{A} \in [0,1]$, $\underline{f'}(\zeta, \tilde{A}) \leq \overline{f'}(\zeta, \tilde{A})$ in both $Tri\mathcal{N}_{number}$ and $Trap\mathcal{N}_{number}$.

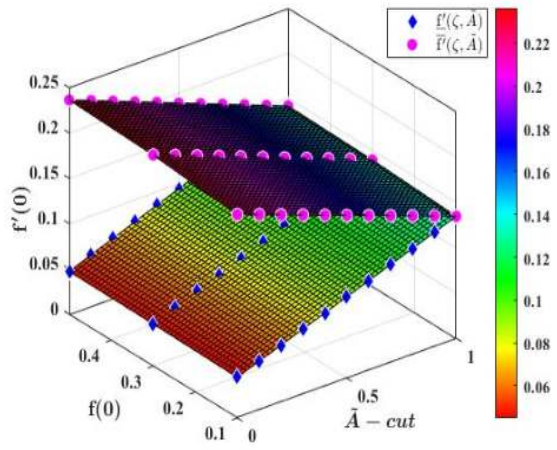

Figure 4. $Tri\mathcal{N}$ velocity for $f(0)$ at $\zeta = 3$

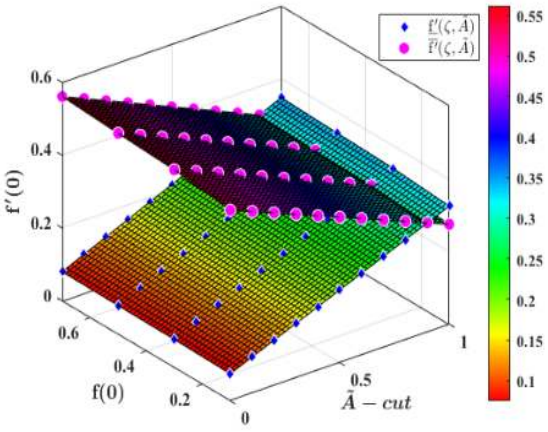

Figure 5. $Trap\mathcal{N}$ velocity for $f(0)$ at $\zeta = 3$

From Figure 6 and 7, we see that $\underline{f'}(\zeta,\widetilde{B})$ is decreasing and $\overline{f'}(\zeta,\widetilde{B})$ is increasing for all $\widetilde{B} \in [0,1]$, $\underline{f'}(\zeta,\widetilde{B}) \leq \overline{f'}(\zeta,\widetilde{B})$ in both $Tri\mathcal{N}_{number}$ and $Trap\mathcal{N}_{number}$ which implies that neutrosophic solution exist.

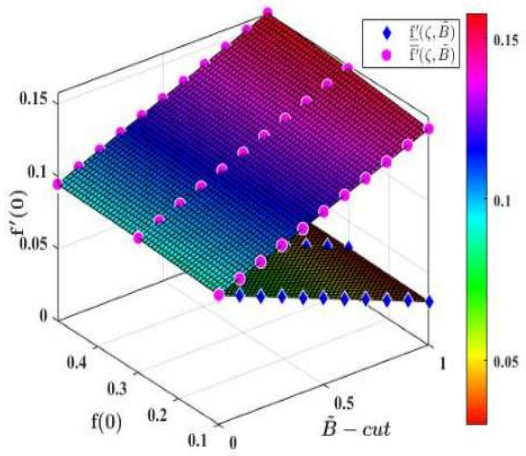

Figure 6. $Tri\mathcal{N}$ velocity for $f(0)$ at $\zeta = 3$

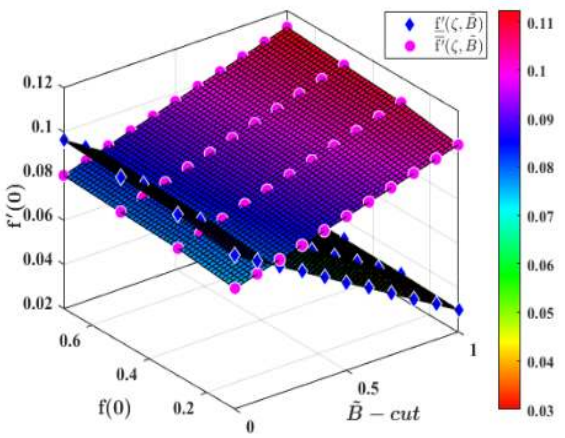

Figure 7. $Trap\mathcal{N}$ velocity for $f(0)$ at $\zeta = 3$

From Figure 8 and 9, it shows that $\underline{f'}(\zeta,\tilde{\Gamma})$ is decreasing and $\overline{f'}(\zeta,\tilde{\Gamma})$ is increasing for all $\tilde{\Gamma} \in [0,1]$, $\underline{f'}(\zeta,\tilde{\Gamma}) \leq \overline{f'}(\zeta,\tilde{\Gamma})$ in both $Tri\mathcal{N}_{number}$ and $Trap\mathcal{N}_{number}$. Hence by Definition 2.9, the solution of (3.6), $f'(\zeta,\tilde{A},\widetilde{B},\tilde{\Gamma})$ is a strong neutrosophic solution.

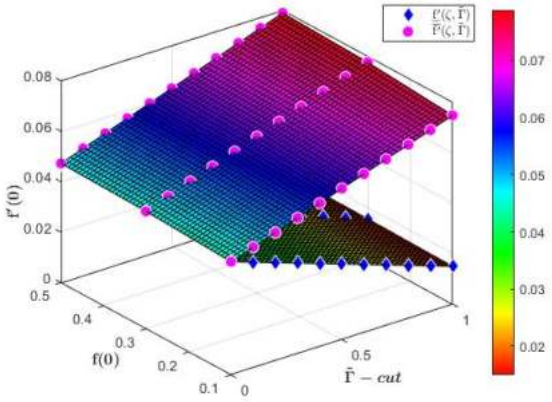

Figure 8. $Tri\mathcal{N}$ velocity for $f(0)$ at $\zeta = 3$

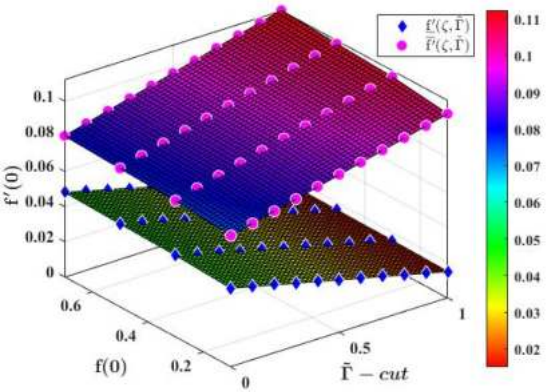

Figure 9. $Trap\mathcal{N}$ velocity for $f(0)$ at $\zeta = 3$

From Figure 10 and 11, we see that $\underline{f'}(\zeta,\widetilde{A})$ is increasing and $\overline{f'}(\zeta,\widetilde{A})$ is decreasing for all $\widetilde{A} \in [0,1]$, $\underline{f'}(\zeta,\widetilde{A}) \leq \overline{f'}(\zeta,\widetilde{A})$ in both $Tri\mathcal{N}_{number}$ and $Trap\mathcal{N}_{number}$.

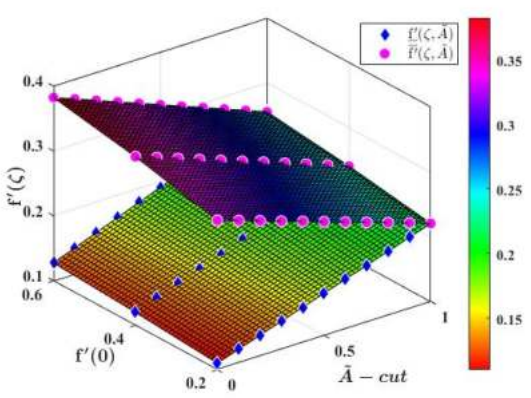

Figure 10. $Tri\mathcal{N}$ velocity for $f'(0)$ at $\zeta = 3$

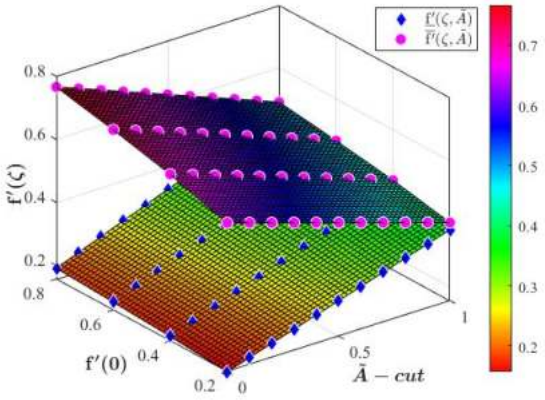

Figure 11. $Trap\mathcal{N}$ velocity for $f'(0)$ at $\zeta = 3$

From Figure 12 and 13, we see that $\underline{f}'(\zeta,\tilde{B})$ is decreasing and $\overline{f}'(\zeta,\tilde{B})$ is increasing for all $\tilde{B} \in [0,1]$, $\underline{f}'(\zeta,\tilde{B}) \leq \overline{f}'(\zeta,\tilde{B})$ in both $Tri\mathcal{N}_{number}$ and $Trap\mathcal{N}_{number}$ which implies that neutrosophic solution exist.

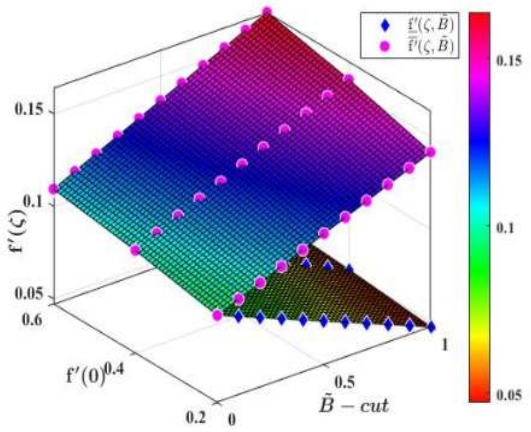

Figure 12. $Tri\mathcal{N}$ velocity for $f'(0)$ at $\zeta = 3$

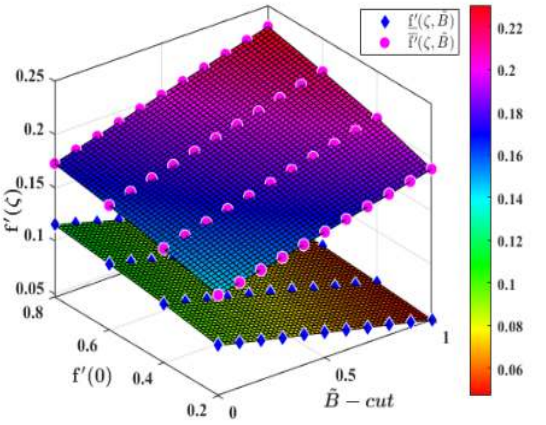

Figure 13. $Trap\mathcal{N}$ velocity for $f'(0)$ at $\zeta = 3$

From Figure 14 and 15, it shows that $\underline{f}'(\zeta,\tilde{\Gamma})$ is decreasing and $\overline{f}'(\zeta,\tilde{\Gamma})$ is increasing for all $\tilde{\Gamma} \in [0,1]$, $\underline{f}'(\zeta,\tilde{\Gamma}) \leq \overline{f}'(\zeta,\tilde{\Gamma})$ in both $Tri\mathcal{N}_{number}$ and $Trap\mathcal{N}_{number}$. Hence by Definition 2.9, the solution of (3.6), $f'(\zeta,\tilde{A},\tilde{B},\tilde{\Gamma})$ is a strong neutrosophic solution.

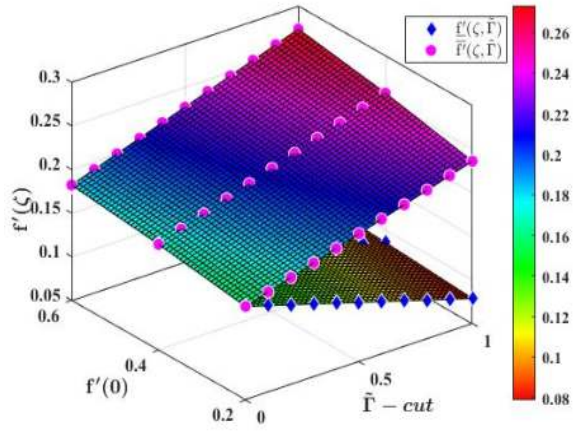

Figure 14. $Tri\mathcal{N}$ velocity for $f'(0)$ at $\zeta = 3$

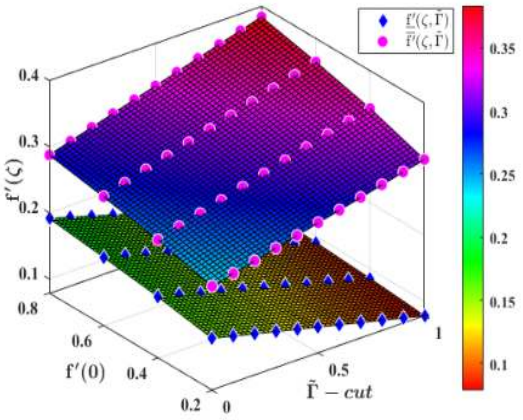

Figure 15. $Trap\mathcal{N}$ velocity for $f'(0)$ at $\zeta = 3$

Case 2: Wedge angle parameter $\tilde{\lambda}$ as $\mathcal{N}_{number}$

Figure 16 and 17 depicts the neutrosophic velocity profiles $f'(\zeta, \tilde{A})$ corresponding to the truth component of the $\mathcal{N}_{number}$. The wedge angle parameter $\tilde{\lambda}$ is taken as $Tri\mathcal{N}_{number}$ [0.2, 0.4, 0.6;0.7, 0.3, 0.5] and $Trap\mathcal{N}_{number}$ [0.2, 0.4, 0.6, 0.8;0.7, 0.3, 0.5] in the Falkner-Skan equation at fixed $\zeta = 3$. The velocity profiles are plotted along the x-axis represents the various cuts $\tilde{A}, \tilde{B}, \tilde{\Gamma}$, the y-axis corresponds to the uncertainty parameter ζ, and the z-axis represents $f'(\zeta, \tilde{A})$. The figures shows that $\underline{f'}(\zeta, \tilde{A})$ is strictly increasing and $\overline{f'}(\zeta, \tilde{A})$ is strictly decreasing for all $\tilde{A} \in [0,1]$, $\underline{f'}(\zeta, \tilde{A}) \leq \overline{f'}(\zeta, \tilde{A})$ in both $Tri\mathcal{N}_{number}$ and $Trap\mathcal{N}_{number}$.

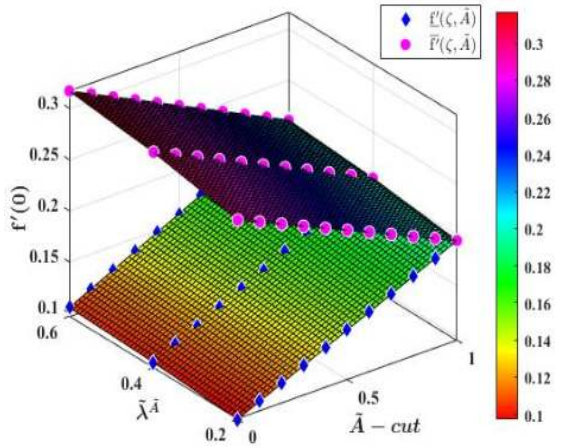

Figure 16. $Tri\mathcal{N}$ velocity for $truth_{function}$ at $\zeta = 3$

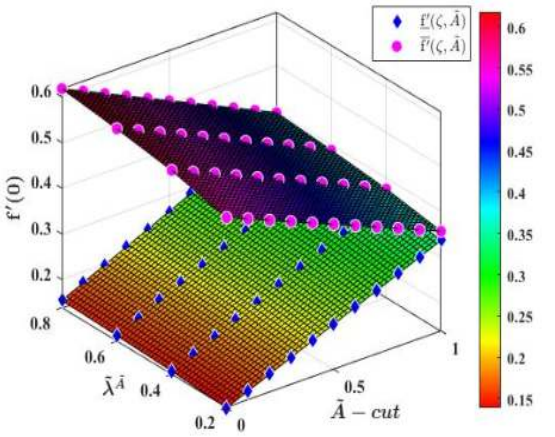

Figure 17. $Trap\mathcal{N}$ velocity for $truth_{function}$ at $\zeta = 3$

From Figure 18 and 19 illustrates that the neutrosophic velocity profile focusing on the indeterminacy. We see that $\underline{f}'(\zeta, \widetilde{B})$ is strictly decreasing and $\overline{f}'(\zeta, \widetilde{B})$ is strictly increasing for all $\widetilde{B} \in [0,1]$, $\underline{f}'(\zeta, \widetilde{B}) \leq \overline{f}'(\zeta, \widetilde{B})$ in both $TriN_{number}$ and $TrapN_{number}$.

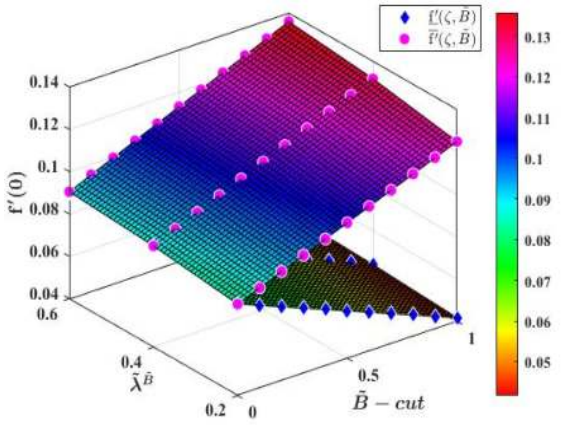

Figure 18. $TriN$ velocity for $indeterministic_{function}$ at $\zeta = 3$

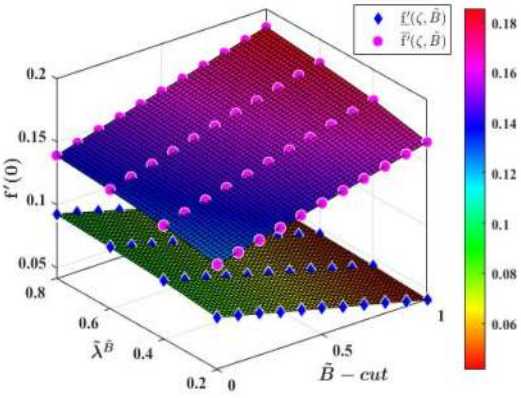

Figure 19. $TrapN$ velocity for $indeterministic_{function}$ at $\zeta = 3$

From Figure 20 and 21 displays $f'(\zeta, \tilde{\Gamma})$ associated with the falsity. It shows that $\underline{f}'(\zeta, \tilde{\Gamma})$ is strictly decreasing and $\overline{f}'(\zeta, \tilde{\Gamma})$ is strictly increasing for all $\tilde{\Gamma} \in [0,1]$, $\underline{f}'(\zeta, \tilde{\Gamma}) \leq \overline{f}'(\zeta, \tilde{\Gamma})$ in both $TriN_{number}$ and $TrapN_{number}$. Hence by Definition 2.9, the solution of (3.6), $f'(\zeta, \tilde{A}, \widetilde{B}, \tilde{\Gamma})$ is a strong neutrosophic solution.

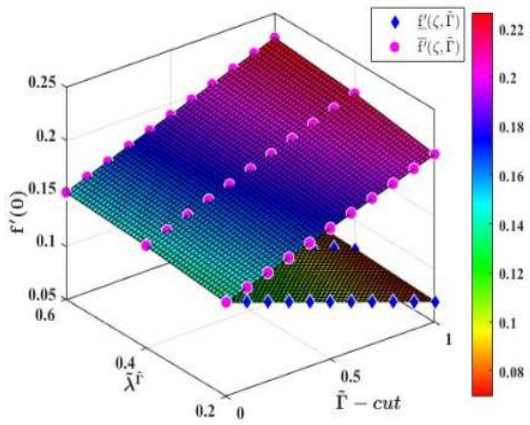

Figure 20. $TriN$ velocity for $falsity_{function}$ at $\zeta = 3$

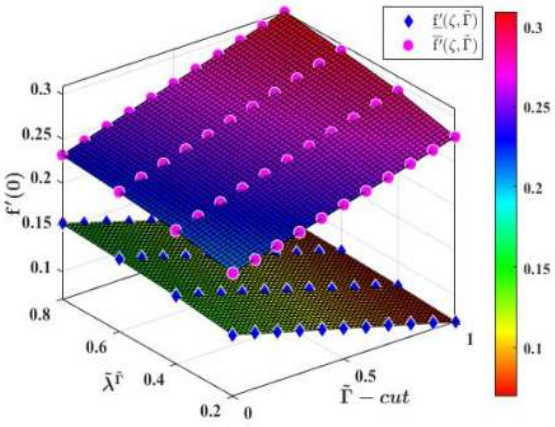

Figure 21. $TrapN$ velocity for $falsity_{function}$ at $\zeta = 3$

5.2 Profile graph of Falkner-Skan Equation via HPM

The velocity profile of $\tilde{\lambda}$ is displayed in Figure 22. The velocity profiles steepen near the wall, indicating that the flow accelerates more rapidly with higher $\tilde{\lambda}$ values. This behavior is attributed to

the enhanced favorable pressure gradient associated with larger $\tilde{\lambda}$ values, which effectively accelerates the fluid particles adjacent to the surface.

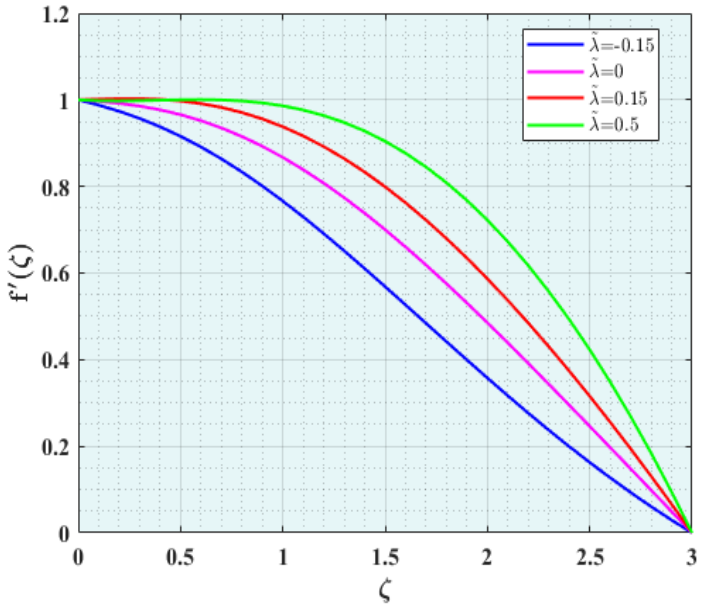

Figure 22. Behavior of $f'(\zeta)$ against $\tilde{\lambda}$

5.2.1 Neutrosophic Analysis using HPM

Case 1: No slip condition as $\mathcal{N}_{number}$

The no slip conditions are taken as $Tri\mathcal{N}_{number}$ and $Trap\mathcal{N}_{number}$. From Figure 23 and 24, we see that $\underline{f'}(\zeta, \tilde{A})$ is increasing and $\overline{f'}(\zeta, \tilde{A})$ is decreasing for all $\tilde{A} \in [0,1]$, $\underline{f'}(\zeta, \tilde{A}) \leq \overline{f'}(\zeta, \tilde{A})$ in both $Tri\mathcal{N}_{number}$ and $Trap\mathcal{N}_{number}$.

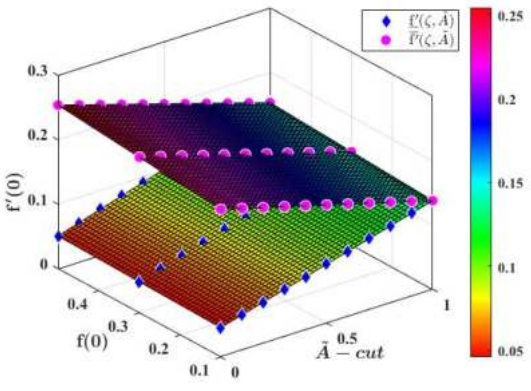

Figure 23. $Tri\mathcal{N}$ velocity for $f(0)$ at $\zeta = 3$

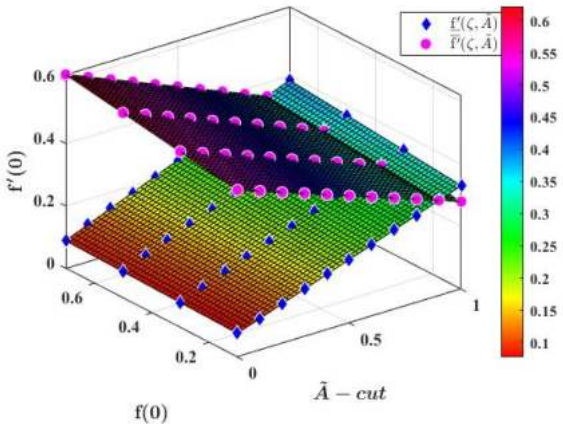

Figure 24. $Trap\mathcal{N}$ velocity for $f(0)$ at $\zeta = 3$

From Figure 25 and 26, we see that $\underline{f'}(\zeta, \widetilde{B})$ is decreasing and $\overline{f'}(\zeta, \widetilde{B})$ is increasing for all $\widetilde{B} \in [0,1]$, $\underline{f'}(\zeta, \widetilde{B}) \leq \overline{f'}(\zeta, \widetilde{B})$ in both $Tri\mathcal{N}_{number}$ and $Trap\mathcal{N}_{number}$ which implies that neutrosophic solution exist.

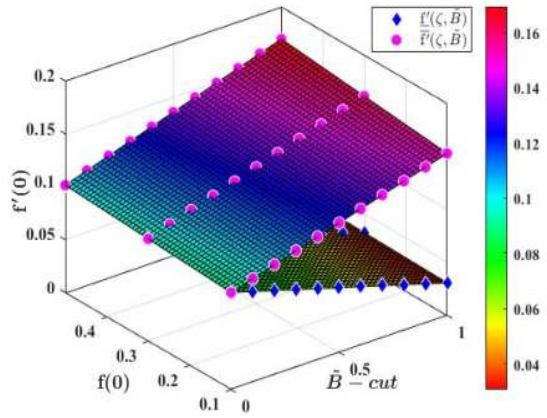

Figure 25. $Tri\mathcal{N}$ velocity for $f(0)$ at $\zeta = 3$

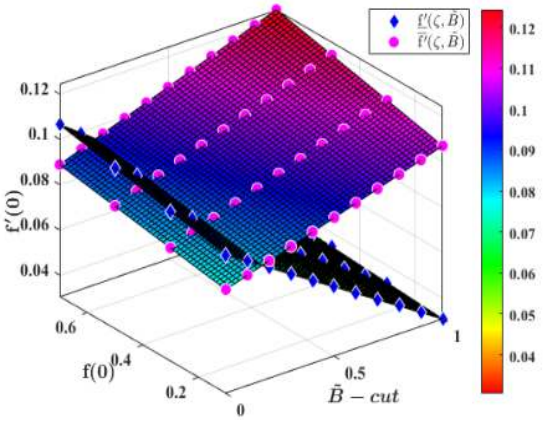

Figure 26. $Trap\mathcal{N}$ velocity for $f(0)$ at $\zeta = 3$

From Figure 27 and 28, it shows that $\underline{f'}(\zeta, \tilde{\Gamma})$ is decreasing and $\overline{f'}(\zeta, \tilde{\Gamma})$ is increasing for all $\tilde{\Gamma} \in [0,1]$, $\underline{f'}(\zeta, \tilde{\Gamma}) \leq \overline{f'}(\zeta, \tilde{\Gamma})$ in both $Tri\mathcal{N}_{number}$ and $Trap\mathcal{N}_{number}$. Hence by Definition 2.9, the solution of (3.6), $f'(\zeta, \tilde{A}, \widetilde{B}, \tilde{\Gamma})$ is a strong neutrosophic solution.

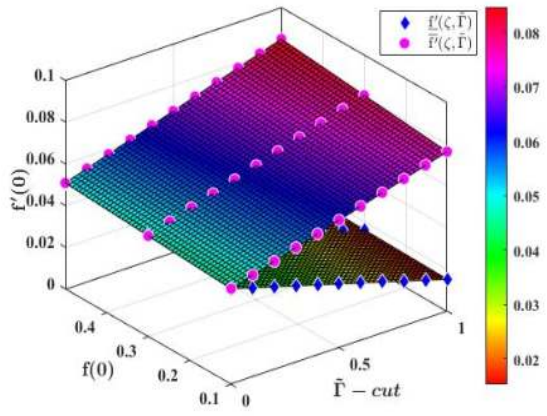

Figure 27. $Tri\mathcal{N}$ velocity for $f(0)$ at $\zeta = 3$

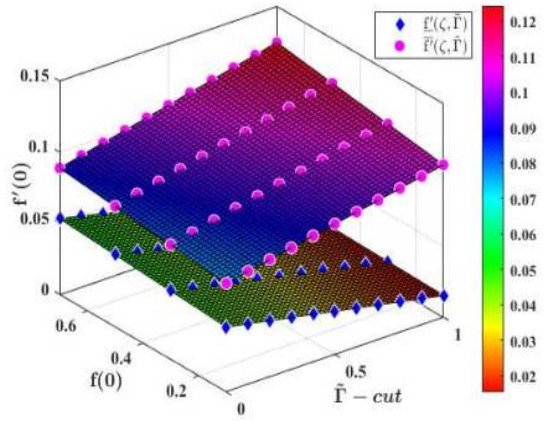

Figure 28. $Trap\mathcal{N}$ velocity for $f(0)$ at $\zeta =$

From Figure 29 and 30, we see that $\underline{f'}(\zeta, \widetilde{A})$ is increasing and $\overline{f'}(\zeta, \widetilde{A})$ is decreasing for all $\widetilde{A} \in [0,1]$, $\underline{f'}(\zeta, \widetilde{A}) \leq \overline{f'}(\zeta, \widetilde{A})$ in both $Tri\mathcal{N}_{number}$ and $Trap\mathcal{N}_{number}$.

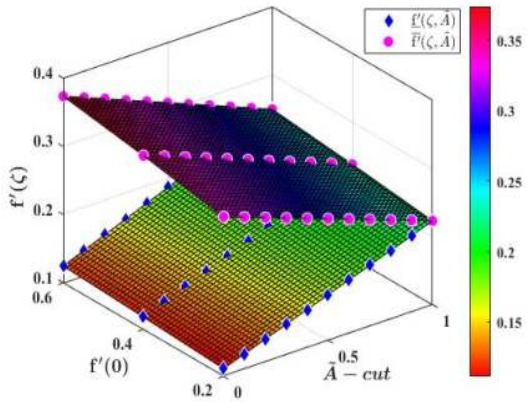

Figure 29. $Tri\mathcal{N}$ velocity for $f'(0)$ at $\zeta = 3$

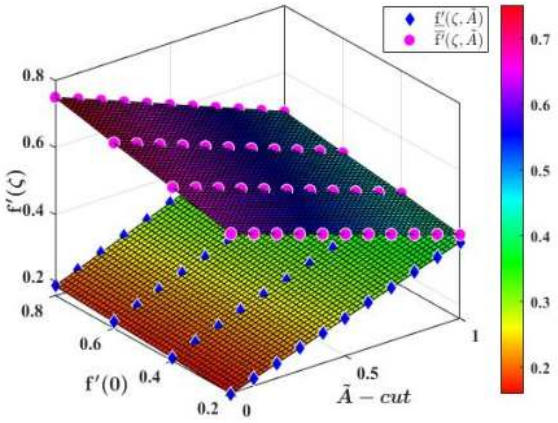

Figure 30. $Trap\mathcal{N}$ velocity for $f'(0)$ at $\zeta = 3$

From Figure 31 and 32, we see that $\underline{f}'(\zeta,\tilde{B})$ is decreasing and $\overline{f}'(\zeta,\tilde{B})$ is increasing for all $\tilde{B} \in [0,1]$, $\underline{f}'(\zeta,\tilde{B}) \leq \overline{f}'(\zeta,\tilde{B})$ in both $Tri\mathcal{N}_{number}$ and $Trap\mathcal{N}_{number}$ which implies that neutrosophic solution exist.

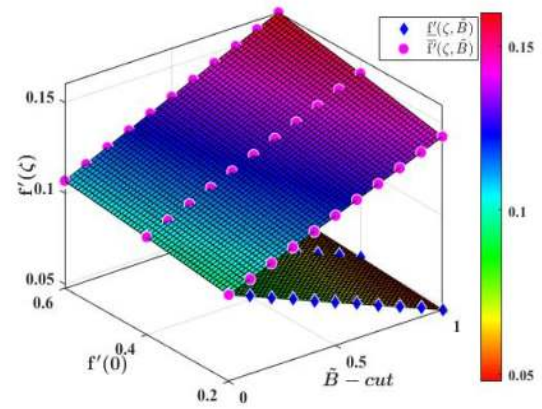

Figure 31. $Tri\mathcal{N}$ velocity for $f'(0)$ at $\zeta = 3$

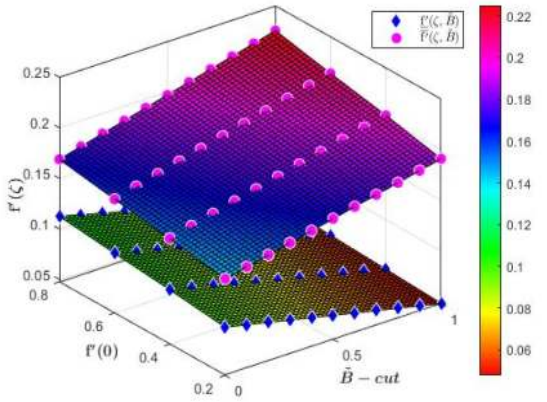

Figure 32. $Trap\mathcal{N}$ velocity for $f(0)$ at $\zeta = 3$

From Figure 33 and 34, it shows that $\underline{f}'(\zeta,\tilde{\Gamma})$ is decreasing and $\overline{f}'(\zeta,\tilde{\Gamma})$ is increasing for all $\tilde{\Gamma} \in [0,1]$, $\underline{f}'(\zeta,\tilde{\Gamma}) \leq \overline{f}'(\zeta,\tilde{\Gamma})$ in both $Tri\mathcal{N}_{number}$ and $Trap\mathcal{N}_{number}$. Hence by Definition 2.9, the solution of (3.6), $f'(\zeta,\tilde{A},\tilde{B},\tilde{\Gamma})$ is a strong neutrosophic solution.

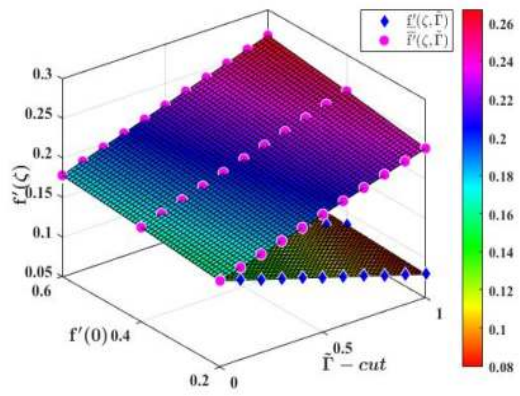

Figure 33. $Tri\mathcal{N}$ velocity for $f(0)$ at $\zeta = 3$

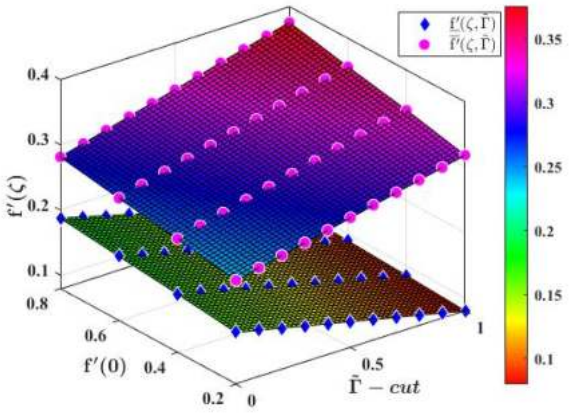

Figure 34. $Trap\mathcal{N}$ velocity for $f(0)$ at $\zeta = 3$

Case 2: Wedge angle parameter $\tilde{\lambda}$ as $\mathcal{N}_{number}$

Figure 35 and 36 demonstrates $f'(\zeta, \tilde{A})$ derived from the truth aspect of the $\mathcal{N}_{number}$. The analysis reveals that both $Tri\mathcal{N}_{number}$ and $Trap\mathcal{N}_{number}$, $\underline{f}'(\zeta, \tilde{A})$ is strictly increasing and $\overline{f}'(\zeta, \tilde{A})$ is strictly decreasing for all $\tilde{A} \in [0,1]$, $\underline{f}'(\zeta, \tilde{A}) \leq \overline{f}'(\zeta, \tilde{A})$.

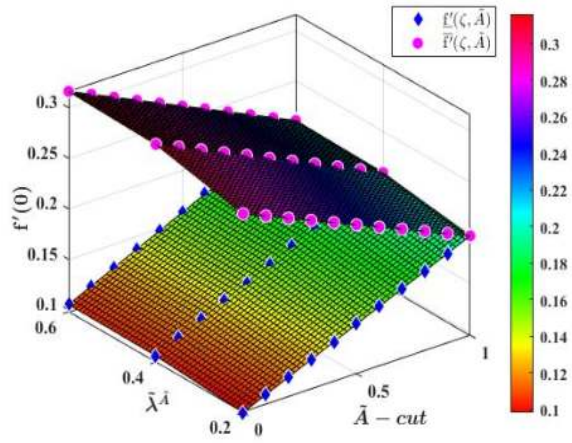

Figure 35. $f'(\zeta, \tilde{A})$ at $\zeta = 3$ using $Tri\mathcal{N}_{number}$

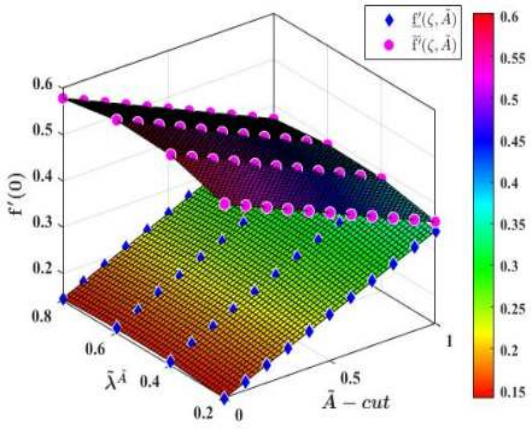

Figure 36. $f'(\zeta, \tilde{A})$ at $\zeta = 3$ using $Trap\mathcal{N}_{number}$

From Figure 37 and 38 showcases the neutrosophic velocity profile corresponding to the indeterminacy aspect. In both $Tri\mathcal{N}_{number}$ and $Trap\mathcal{N}_{number}$ we see that $\underline{f}'(\zeta, \tilde{B})$ is strictly decreasing and $\overline{f}'(\zeta, \tilde{B})$ is strictly increasing for all $\tilde{B} \in [0,1]$, $\underline{f}'(\zeta, \tilde{B}) \leq \overline{f}'(\zeta, \tilde{B})$.

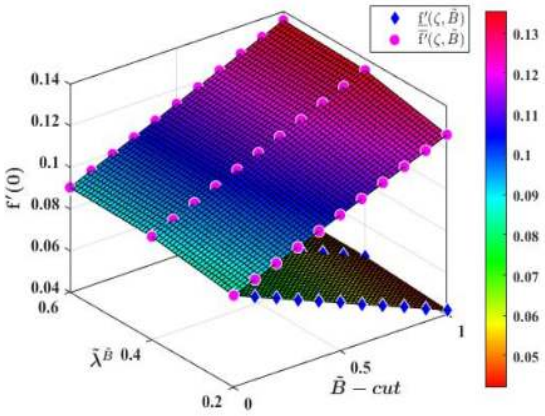

Figure 37. $f'(\zeta,\widetilde{\mathrm{B}})$ at $\zeta=3$ using $Tri\mathcal{N}_{number}$

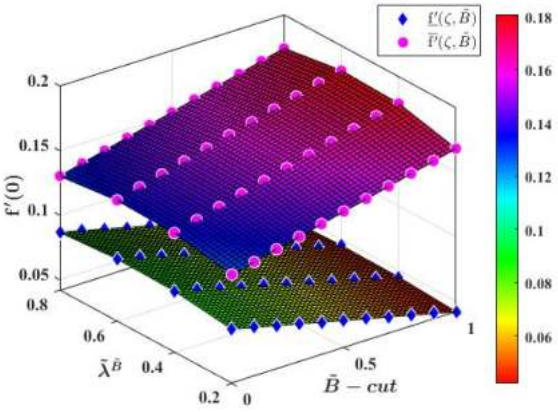

Figure 38. $f'(\zeta,\widetilde{\mathrm{B}})$ at $\zeta=3$ using $Trap\mathcal{N}_{number}$

From Figure 39 and 40 presents the neutrosophic velocity profile related to the falsity aspect. Similar to the observations made for indeterminacy, the $Tri\mathcal{N}_{number}$ and $Trap\mathcal{N}_{number}$ reveals that $\underline{f}'(\zeta,\tilde{\Gamma})$ is strictly decreasing and $\overline{f}'(\zeta,\tilde{\Gamma})$ is strictly increasing for all $\tilde{\Gamma}\in[0,1]$, $\underline{f}'(\zeta,\tilde{\Gamma})\le\overline{f}'(\zeta,\tilde{\Gamma})$. Hence by Definition 2.9, the solution of (3.6), $f'(\zeta,\tilde{A},\widetilde{\mathrm{B}},\tilde{\Gamma})$ is a strong neutrosophic solution.

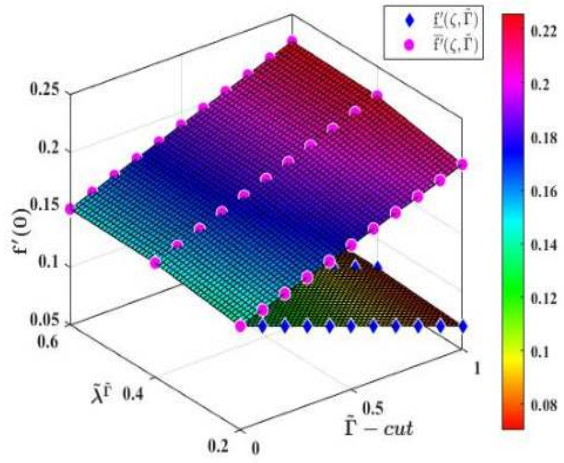

Figure 39. $f'(\zeta,\tilde{\Gamma})$ at $\zeta=3$ using $Tri\mathcal{N}_{number}$

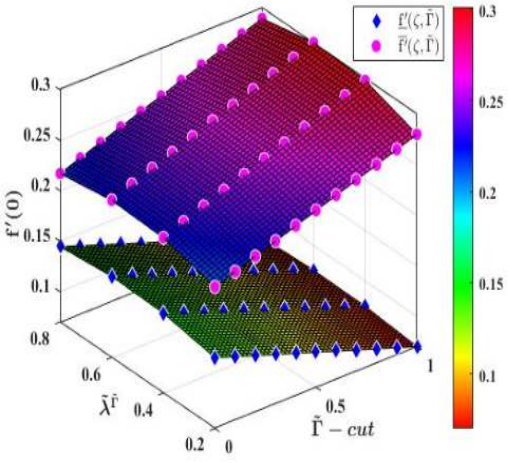

Figure 40. $f'(\zeta,\tilde{\Gamma})$ at $\zeta=3$ using $Trap\mathcal{N}_{number}$

5.3 Comparison of Shooting method and HPM

We computed the absolute error between the values obtained from the Shooting method and the HPM for the $Tri\mathcal{N}_{number}$ and $Trap\mathcal{N}_{number}$. The absolute errors were computed separately for each $(\widetilde{\mathrm{A}},\widetilde{\mathrm{B}},\tilde{\Gamma})_{cut}$. These errors were then visualized in a 3D plot, with the x-axis represents the cuts $\tilde{A},\widetilde{\mathrm{B}},\tilde{\Gamma}$, the y-axis corresponds to the uncertainty parameter $\tilde{\lambda}$, and the z-axis represents the absolute error. The analysis demonstrates that the choice between $Tri\mathcal{N}_{number}$and $Trap\mathcal{N}_{number}$ impacts the

resulting velocity profiles significantly. Based on the results, $Tri\mathcal{N}_{number}$ and $Trap\mathcal{N}_{number}$ exhibits lower errors at higher cuts.

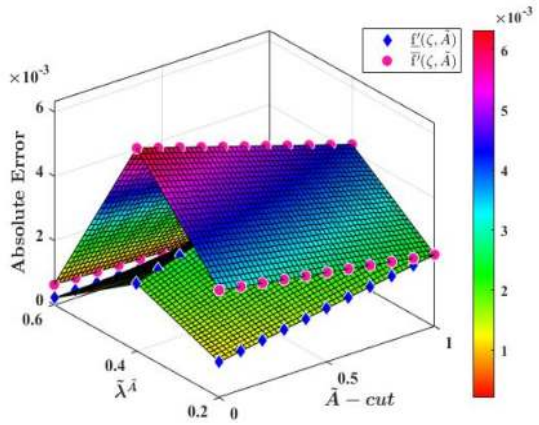

Figure 41. Absolute Error of $f'(\zeta, \tilde{A})$ using $Tri\mathcal{N}_{number}$

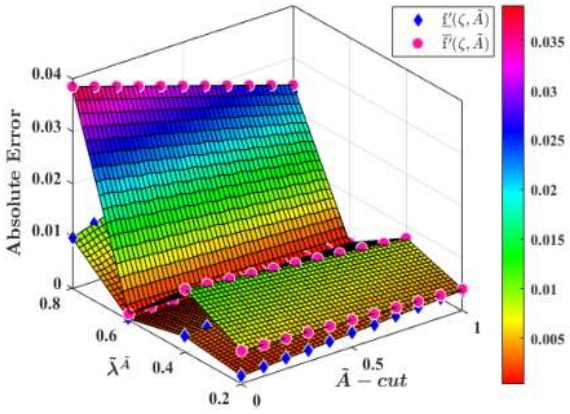

Figure 42. Absolute Error of $f'(\zeta, \tilde{A})$ using $Trap\mathcal{N}_{number}$

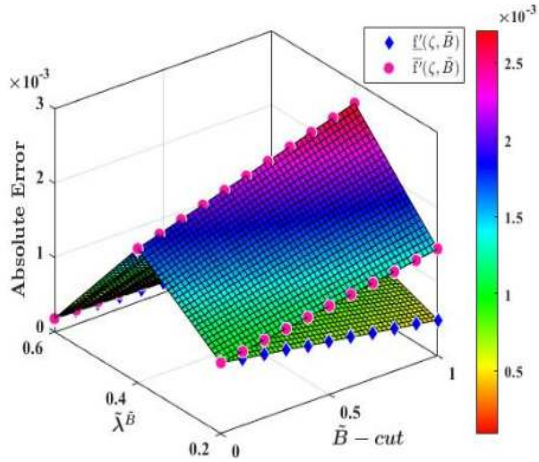

Figure 43. Absolute Error of $f'(\zeta, \tilde{B})$ using $Tri\mathcal{N}_{number}$

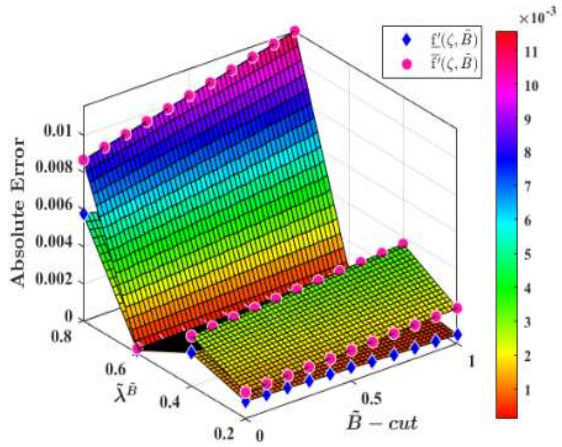

Figure 44. Absolute Error of $f'(\zeta, \tilde{B})$ using $Trap\mathcal{N}_{number}$

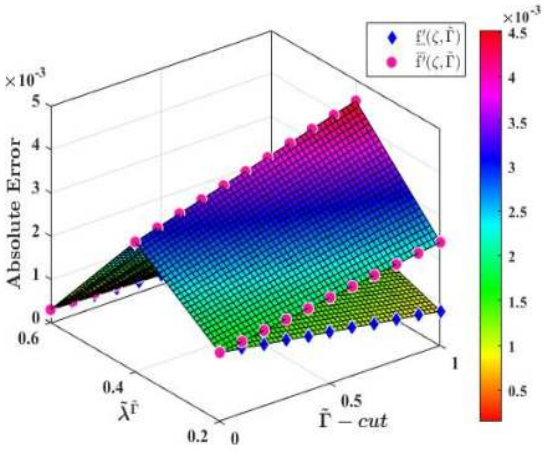

Figure 45. Absolute Error of $f'(\zeta, \tilde{\Gamma})$ using $TriN_{number}$

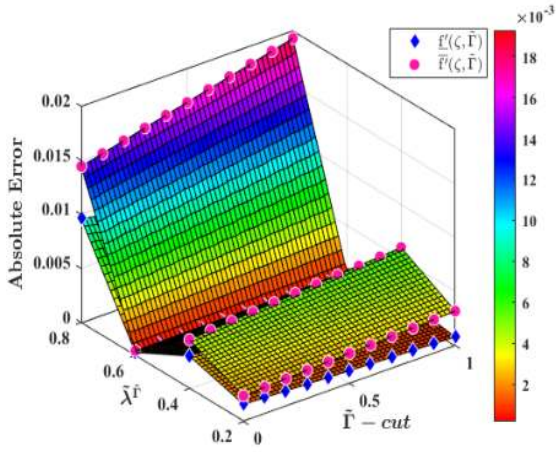

Figure 46. Absolute Error of $f'(\zeta, \tilde{\Gamma})$ using $TrapN_{number}$

The results, as shown in Table 4, indicate that the $TrapN_{number}$ exhibits higher truth mean values for both shooting method and HPM. However, the $TriN_{number}$consistently shows lower mean indeterminacy and falsity values. $TriN_{number}$ gives a better performance in minimizing uncertainty and falsity. The Shooting Method slightly outperforms HPM in achieving a higher truth value for both types of N_{number}. The Shooting Method shows slightly lower indeterminacy for both types, indicates better performance in minimizing uncertainty. The Shooting Method again results in slightly lower falsity values, it is more effective in minimizing errors.

Table 4. Comparison of Mean Values of Neutrosophic Velocity

	Shooting Method		**HPM**	
	$\boldsymbol{TriN_{number}}$	$\boldsymbol{TrapN_{number}}$	$\boldsymbol{TriN_{number}}$	$\boldsymbol{TrapN_{number}}$
$\widetilde{A}_{cut}$	0.203434	0.368977	0.205443	0.365649
$\widetilde{B}_{cut}$	0.087186	0.110693	0.088047	0.109695
$\widetilde{\Gamma}_{cut}$	0.14531	0.184488	0.146745	0.182824

6. Conclusion

This study focused on neutrosophic analysis of Falkner-Skan boundary layer equation over wedge. The impact of wedge angle parameter $\tilde{\lambda}$ on velocity profile has been studied by employing shooting method and HPM, the NDEs are solved numerically. The wedge parameter $\tilde{\lambda}$ and no slip conditions are considered as $TriN_{number}$ and $TrapN_{number}$ with the help of $(\widetilde{A}, \widetilde{B}, \widetilde{\Gamma})_{cut}$ which control uncertainty. The key outcomes of this study are as follows:

- The velocity profile curve $f'(\zeta)$ upsurge for $\tilde{\lambda}$ in both shooting method and HPM.

- The Shooting Method is considered superior for solving the Falkner-Skan equation under uncertainty with $\tilde{\lambda}$.
- Mean values of $Tri\mathcal{N}_{number}$ and $Tri\mathcal{N}_{number}$ are compared, which show triangular membership function performs better than trapezoidal membership function in reducing uncertainty.
- For both $Tri\mathcal{N}_{number}$ and $Tri\mathcal{N}_{number}$, the error was found to vary significantly across different cuts.
- The neutrosophic concept has been applied to Falkner-Skan equation whose solution follows the conditions of strong neutrosophic solution in both methods.

Funding

This research received no external funding.

Acknowledgments

The authors wish to express gratitude to the Management, Principal and Vice Principal, Sri Sivasubramaniya Nadar College of Engineering, Chennai, India.

Conflicts of Interest

The authors declare no conflicts of interest.

References

1. Zadeh L.A. (1965). Fuzzy sets. Information and control, 8(3), 338-353.
2. Atanassov K.T. (1999). Intuitionistic Fuzzy Sets: Theory and Applications, vol. 35. Studies in Fuzziness and Soft Computing.
3. Atanassov K.T. (2000). Two theorems for intuitionistic fuzzy sets. Fuzzy sets and systems, 110(2), 267-269.
4. Atanassov K.T. (2003, September). Intuitionistic fuzzy sets: past, present and future. In EUSFLAT Conf. (pp. 12-19).
5. Atanassov K.T. (2016). Intuitionistic fuzzy sets. International journal bio automation, 20, 1.
6. Smarandache F. (2002, January). Neutrosophy and neutrosophic logic. In First international conference on neutrosophy, neutrosophic logic, set, probability, and statistics university of New Mexico, Gallup, NM (Vol. 87301, pp. 338-353).
7. Wang H, Smarandache F, Sunderraman R, Zhang Y.Q. (2005). interval neutrosophic sets and logic: theory and applications in computing: Theory and applications in computing (Vol. 5). Infinite Study.
8. Smarandache F. (2010). Neutrosophic set–a generalization of the intuitionistic fuzzy set. Journal of Defense Resources Management (JoDRM), 1(1), 107-116.
9. Bede B, Rudas I.J, Bencsik A.L. (2007). First order linear fuzzy differential equations under generalized differentiability. Information sciences, 177(7), 1648-1662.
10. Vasavi C.H, Kumar G.S, Rao T.S, Rao B.A. (2017). Application of fuzzy differential equations for cooling problems. International Journal of Mechanical Engineering and Technology, 8(12), 712-721.

11. Ettoussi R, Melliani S, Elomari M, Chadli L.S. (2015). Solution of intuitionistic fuzzy differential equations by successive approximations method. Notes on Intuitionistic Fuzzy Sets, 21(2), 51-62.
12. Moi S, Biswas S, Pal S. (2021). Second-order neutrosophic boundary-value problem. Complex and Intelligent Systems, 7, 1079-1098.
13. Broumi S, Sundareswaran R, Shanmugapriya M, Singh P.K, Voskoglou M, Talea M. (2023). Faculty performance evaluation through multi-criteria decision analysis using interval-valued fermatean neutrosophic sets. Mathematics, 11(18), 3817.
14. Acharya A, Mahata A, Mukherjee S, Biswas M.A, Das K.P, Mondal S.P, Roy B. (2023). A Neutrosophic differential equation approach for modelling glucose distribution in the bloodstream using neutrosophic sets. Decision Analytics Journal, 8, 100264.
15. Chai J.S, Selvachandran G, Smarandache F, Gerogiannis V.C, Son L.H, Bui Q.T, Vo B. (2021). New similarity measures for single-valued neutrosophic sets with applications in pattern recognition and medical diagnosis problems. Complex Intelligent Systems, 7, 703-723.
16. Mondal D, Tudu S, Roy G.C, Roy T.K. (2021). A model describing the neutrosophic differential equation and its application on mine safety. Neutrosophic Sets System, 46, 386-401.
17. Parikh M, Sahni M. (2024). Solution of logistic differential equation in an uncertain environment using neutrosophic numbers. Journal of Interdisciplinary Mathematics, 27, 145-169.
18. Bhaumik A, Roy S.K, Li D.F. (2021). (α, β, γ)cut set based ranking approach to solving bi-matrix games in neutrosophic environment. Soft Computing, 25, 2729-2739.
19. Shanmugapriya M, Sundareswaran R, Broumi S.S. (2023) Solution and Analysis of System of Differential Equation with Initial Condition as TrapNnumber. Neutrosophic Sets and Systems, 57(1) 194-209.
20. Han S. (2013). Finite Difference Solution of the Falkner—Skan Wedge Flow Equation. International Journal of Mechanical Engineering Education, 41(1), 1-7.
21. Parand K, Dehghan M, Pirkhedri A. (2012). The use of Sinc-collocation method for solving Falkner–Skan boundary-layer equation. International journal for numerical methods in fluids, 68(1), 36-47.
22. Elnady A.O, Abd Rabbo M.F, Negm H.M. (2020). Solution of the Falkner–Skan equation using the Chebyshev series in matrix form. Journal of Engineering, 2020(1), 3972573.
23. Barania H, Haghparast N, Miansari M, Barari A. (2012). Flow analysis for the Falkner–Skan wedge flow. Current Science, 169-177.
24. Shanmugapriya M, Sundareswaran R, Gopi Krishna S, Alameri A. (2024). Investigation of Magnetized Casson Nanofluid Flow along Wedge: Gaussian Process Regression. International Journal of Mathematics and Mathematical Sciences, 2024(1), 2880748.
25. Shanmugapriya M. (2018). Analysis of Heat Transfer of Cu-Water Nanofluid Flow Past a Moving Wedge. Journal of Informatics and Mathematical Sciences, 10.

26. GopiKrishna S, Shanmugapriya M. (2021). Inquiry of MHD bioconvective non-newtonian nanofluid flow over a moving wedge using HPM. Materials Today: Proceedings, 38, 3297-3305.
27. Zulqarnain R.M, Nadeem M, Siddique I, Ahmad H, Askar S, Samar, M. (2023). Heat transfer analysis of Maxwell tri-hybridized nanofluid through Riga wedge with fuzzy volume fraction. Scientific Reports, 13(1), 18238.
28. Nadeem M, Siddique I, Bilal M, Ali R. (2022). Significance of heat transfer for second-grade fuzzy hybrid nanofluid flow past over a stretching/shrinking riga wedge.
29. Shanmugapriya M, Sundareswaran R, Krishna S.G, Pal, M. (2024). An analysis of effect of higher order endothermic/exothermic chemical reaction on magnetized casson hybrid nanofluid flow using fuzzy triangular number. Engineering Applications of Artificial Intelligence, 133, 108-119.
30. Kamal B, Khalid H.E, Salama A.A, El-Baghdady G.I. (2023). Finite Difference Method for Neutrosophic Fuzzy Second Order Differential Equation under Generalized Hukuhara Differentiability. Neutrosophic Sets and Systems, 58(1), 19.
31. Sumathi I.R, Priya V. M. (2018). A New Perspective on Neutrosophic Differential Equation. International Journal of Engineering and Technology, 7(4.10), 422-425.
32. Sumathi I.R, Antony Crispin Sweety C. (2019). New approach on differential equation via trapezoidal neutrosophic number. Complex and Intelligent Systems, 5, 417-424.
33. Belden E.R, Dickman Z.A, Weinstein S.J, Archibee A.D, Burroughs E, Barlow N.S. (2020). Asymptotic approximant for the Falkner–Skan boundary layer equation. The Quarterly Journal of Mechanics and Applied Mathematics, 73(1), 36-50.
34. Khan I, Ullah H, AlSalman H, Fiza M, Islam S, Zahoor Raja A, Gumaei A.H. (2021). Falkner–Skan equation with heat transfer: A new stochastic numerical approach. Mathematical Problems in Engineering, 2021(1), 3921481.
35. Zhang J, Chen B. (2009). An iterative method for solving the Falkner–Skan equation. Applied Mathematics and Computation, 210(1), 215-222.
36. Salama A.A. (2004). Higher-order method for solving free boundary-value problems. Numerical Heat Transfer, Part B: Fundamentals, 45(4), 385-394.